



Strength and Acid Resistance of Mortar with Different Binders from Palm Oil Fuel Ash, Slag, and Calcium Carbide Residue

Akkadath Abdulmatin ¹, Nurihan Sa ², Saofee Dueramae ^{3*},
Sattawat Haruehansapong ⁴, Weerachart Tangchirapat ², Chai Jaturapitakkul ²

¹ Department of Civil Engineering, Faculty of Engineering, Princess of Naradhiwas University (PNU), Naradhiwas 96000, Thailand.

² Department of Civil Engineering, Faculty of Engineering, King Mongkut's University of Technology Thonburi (KMUTT), Bangkok 10140, Thailand.

³ Department of Civil Engineering, Faculty of Engineering, Rajamangala University of Technology Krungthep (RMUTK), Bangkok 10120, Thailand.

⁴ Department of Civil Engineering, Faculty of Engineering and Architecture, Rajamangala University of Technology Tawan-Ok, Uthenthawai Campus, Bangkok, 10330, Thailand.

Received 07 March 2024; Revised 25 May 2024; Accepted 06 June 2024; Published 01 July 2024

Abstract

This study deals with the use of ground palm oil fuel ash (GPOFA) in combination with ground granulated blast furnace slag (GGBFS) and ground calcium carbide residue (GCR) to produce the binary and ternary binders-based alkali activated mortar. The appropriate content of materials in each binder type was determined as a function of compressive strength. The results revealed that both GPOFA:GGBFS and GPOFA:GCR binders had an optimum blending ratio of 70:30 wt%, while the GPOFA:GGBFS:GCR binder was 55:30:15 wt%. An alkaline catalyst of NaOH was admixed to the best mixture in each binder type to stimulate the mortar's compressive strength. The sulfuric acid (H₂SO₄) resistance of the mortar in terms of weight change was also examined. The addition of 1M NaOH in both binary and ternary binders could enhance the compressive strength and H₂SO₄ resistance of the mortar. The highest compressive strength and lowest weight change due to soaking in H₂SO₄ solution were found in the ternary binder mortar with a 1 M NaOH. The mortar with GCR immersed in H₂SO₄ solution resulted in an increased weight, which was different from that of the mortar without GCR. The microstructural analysis of the alkali-activated pastes indicated more reaction products than in the case of the pastes without alkali activator. However, a higher concentration of 2 M NaOH resulted in a poor microstructure, which had a negative effect on the compressive strength and H₂SO₄ resistance.

Keywords: Calcium Carbide Residue; Granulated Blast Furnace Slag; Palm Oil Fuel Ash; Alkali Activated Mortar; Sulfuric Acid Resistance.

1. Introduction

The conservation of natural resources and the reduction of greenhouse gas emissions are currently being widely discussed around the world. The cement industry is one of the segments with high consumption of natural resources and high greenhouse gas emissions. Emissions from cement production account for about 6% of anthropogenic activities [1]. Therefore, the utilization of pozzolans from industrial wastes such as fly ash (FA), coal bottom ash (CBA), bagasse ash (BA), and palm oil fuel ash (POFA) can now be used as cement replacement materials. However, the use of various pozzolanic materials must require a part of cement to be included in the mixture. Currently, studies are being focused on the 100% replacement of cement with an alternative binder for use as a cementing material. The use of pozzolanic materials mixed with calcium-rich materials such as granulated blast furnace slag (GBFS) or calcium carbide residue (CCR) is a cement-free binder that has the potential to replace cement.

* Corresponding author: saofee.d@mail.rmutk.ac.th

<http://dx.doi.org/10.28991/CEJ-2024-010-07-08>



© 2024 by the authors. Licensee C.E.J, Tehran, Iran. This article is an open access article distributed under the terms and conditions of the Creative Commons Attribution (CC-BY) license (<http://creativecommons.org/licenses/by/4.0/>).

In Thailand, about 300,000 tons of POFA are produced annually [2], and the trend is increasing every year. Thus, the use of POFA to produce cementitious material is a good way to reduce the amount of this agricultural waste. POFA is acceptable as a pozzolan to partially replace cement when its fineness is increased. The chemical properties of POFA depend on the nature of the raw product before combustion, the temperature, and the conditions of combustion. Safiuddin et al. [3] summarized that the chemical composition of POFA was mainly silicon dioxide (SiO_2) with a proportion of 44–66%, while the proportions of aluminum oxide (Al_2O_3) and calcium oxide (CaO) were lower, at 1.5–11.5% and 4.0–8.5%, respectively. Some research [4–7] addressed the use of ground POFA (GPOFA) in combination with alkali agents as a cementitious material such as geopolymer or alkali activated binder. Most of the literature indicated that the binder prepared from pure GPOFA with alkali activators should be cured by heating to about 65–90 °C. However, the compressive strength was still low, especially at early ages, because the deficiency of alumina content caused a delay in the chemical reaction of aluminosilicate. To solve this problem, the addition of material with a high alumina content, such as FA, was a way to enhance the chemical reaction of aluminosilicate, resulting in an increase in strength [8]. However, a temperature-cured process was still necessary in the geopolymer mixture when adding alumina-rich material. Najimi et al. [9] also mentioned that the alkali-activated binder of low-calcium material was limited in the formation product at ambient temperature, which must be cured at elevated temperature. Therefore, GPOFA that has a low calcium content should be used together with other calcium-rich materials to accelerate the formation of the early solid matrix at ambient temperature, such as calcium silicate hydrate (C-S-H) and calcium aluminosilicate hydrate (C-A-S-H). Two by-products of calcium-rich materials, GBFS and CCR, were used in this study.

In steel or iron production, the iron ore mineral is melted together with limestone and coke at approximately 1500°C, producing steel and slag from the blast furnace. This slag is expeditiously cooled and converted into GBFS [10]. The chemical compositions of GBFS are mainly composed of CaO (30–50%), SiO_2 (30–40%), Al_2O_3 (7–19%), and MgO (3.5–21%) [11, 12]. GBFS is an amorphous material and can therefore be used to partially replace cement or used together with other waste materials as an alkali-activated binder. For instance, Kumar & Mishra [13] investigated the influence of ground GBFS (GGBFS) on the strength of alkali activated concrete. The result showed that increasing the GGBFS content in the alkali-activated fly ash concrete led to a significant increase in the strength of the concrete. Moreover, with the same solid/liquid ratio of 0.5, an alkali activator ratio (sodium silicate; Na_2SiO_3 /sodium hydroxide; NaOH) of 1.8, and a 24-hour heat curing at 60 °C, the alkali activated concrete consisting solely of GGBFS could increase the strength by 245% over an alkali activated fly ash concrete. Similar to the result of Sunarsih et al. [14], they also found that the addition of a slag substituted low calcium fly ash mixture could improve the compressive strength of the fly ash-slag base geopolymer. The optimum content of silica, alumina, and calcium in precursor material was a key factor in chemical reactivity and mechanical properties. Tanu & Unnikrishnan [15] studied the production of alkali-activated concrete from GGBFS and ground BA (GBA), which set the target strength of 30–35 MPa. The information revealed that although the decline in compressive strength of the concrete occurred when the GBA content in the mixture was increased by 0–20% by weight (wt%), the concrete with GGBFS:GBA in the ratio of 80:20 wt% (Na_2SiO_3 / NaOH ratio = 2.5) could achieve the target compressive strength. Moreover, microstructural analysis of the binder from GGBFS and GBA at the higher NaOH concentration of 12 M indicated the alkali-activated product of C-A-S-H.

CCR was another calcium-rich material used in this study. Many studies had shown that CCR in combination with pozzolanic materials could completely replace cement, producing the cementation products from the pozzolanic reaction [16–19]. However, the strength of mortar or concrete from the binder of CCR in combination with pozzolanic materials was low when there was no activation method. Dueramae et al. [20] investigated the mortar prepared from ground CCR (GCR) and ground FA (GFA) using the different activation methods of adding NaOH at 1 wt% of the binder and curing the GCR:GFA mortar at 60 °C for 24 hours. The use of NaOH in the mixture and heat curing produced higher early strength (at 3 days) than non-activated mortar of 11.8 and 19.7 MPa, respectively. However, the use of the heat curing method showed the least development of compressive strength, i.e., the compressive strength after 28 days of the mortar with heat curing was about the same as that of the non-activated mortar, while the mortar with NaOH in the mixture was 9.0 MPa higher than the non-activated mortar. Hanjitsuwan et al. [21] and Suttiwapa et al. [22] inspected GCR combination coal ash, ground CBA (GCBA), and GFA using Na_2SiO_3 and NaOH as alkali catalysts and a constant Na_2SiO_3 / NaOH ratio of 2.0. The results showed that both 70 wt% GCBA and GFA mixed with 30 wt% GCR gave suitable results in terms of compressive strength. Both alkali-activated GCR:GCBA and GCR:FA resulted mainly in C-S-H and C-A-S-H formation.

Based on the previous literature, GPOFA is used in conjunction with two calcium-rich materials, GGBFS and GCR, and has received limited investigation. Therefore, the compressive strength and microstructural analysis of binary and ternary binders composed of GPOFA:GGBFS, GPOFA:GCR, and GPOFA:GGBFS:GCR were investigated, and only NaOH was used as an alkali activator in this study. Moreover, calcium-containing binders can affect the acid resistance of mortar or concrete. In the case of binders with a high calcium content, an electrochemical ion exchange between calcium ions and acid protons (H^+ or H_3O^+) could occur, which leads to the destruction of the structure of the hardened reaction products [23]. In addition, the calcium content in the formation of calcium hydroxide ($\text{Ca}(\text{OH})_2$) could respond to H_2SO_4 , engendering the formation of gypsum [24]. The deposition of gypsum affected the weight gain of the

specimen, and the continuous deposition of gypsum could cause the specimen to crack due to internal stresses [25]. Therefore, the study of the H₂SO₄ resistance of the mortar is essential, since there were no or few studies on these binders for H₂SO₄ resistance, especially binders with CCR in the mixture. It is believed that the results of this study have the potential to reuse industrial waste products as novel binders without Portland cement by utilizing the by-products POFA, GBFS, and CCR to expand the knowledge of concrete technology. This not only reduces the dependence on new natural raw materials but also converts waste into valuable materials.

2. Material and Method

2.1. Methodology Method

Figure 1 summarizes the workflow diagram of the research investigation.

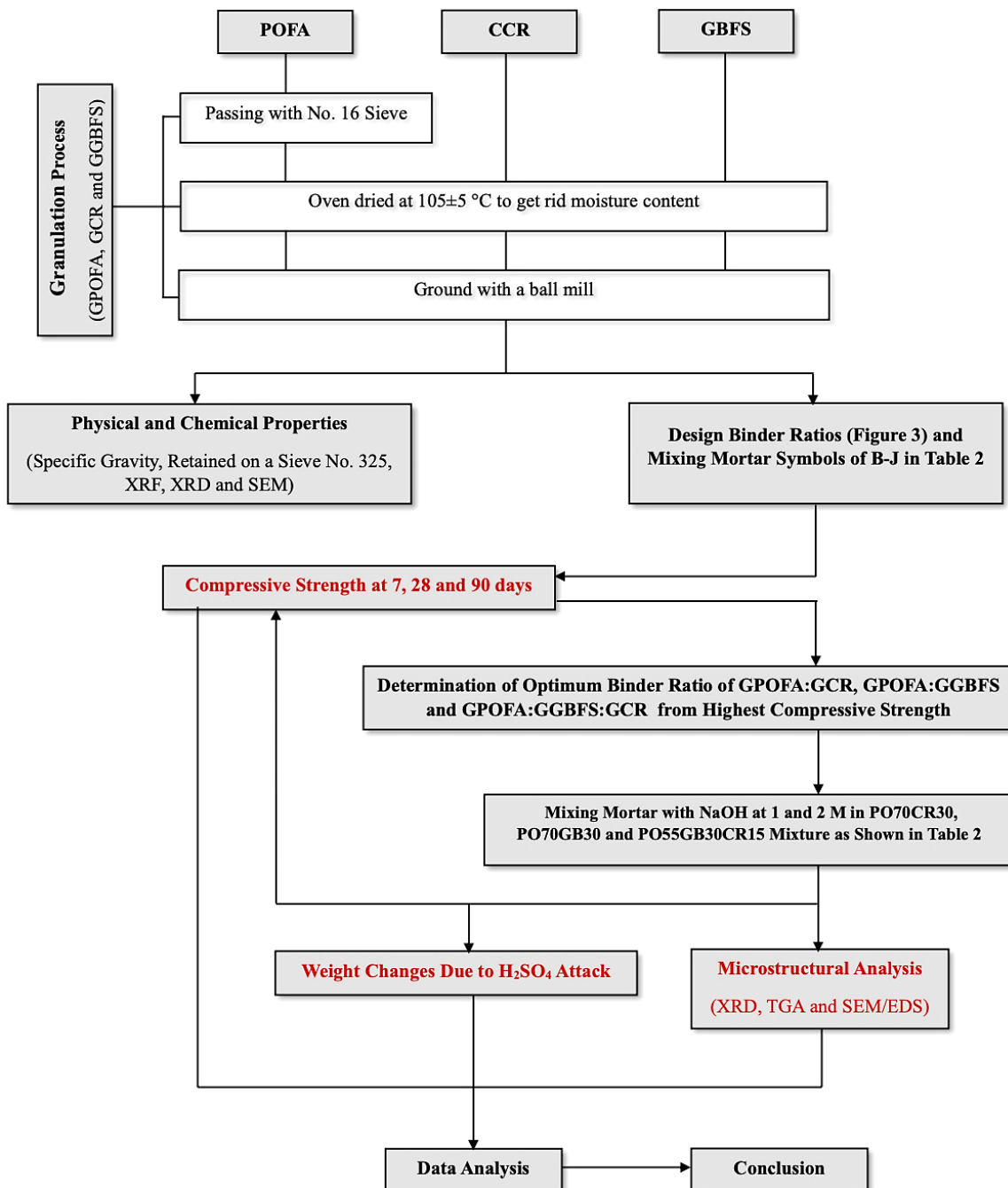


Figure 1. Methodology flow chart

2.2. Materials

In this study, GPOFA, GGBFS, and GCR were used as materials for the preparation of mortars. GPOFA, GGBFS, and GCR exhibited fineness in terms of retained on sieve No. 325 of 0.65, 3.61, and 9.23 wt%, respectively, corresponding to specific gravities of 2.37, 2.95, and 2.58.

Figure 2 shows scanning electron microscope (SEM) images of GPOFA (Figure 2-a), GGBFS (Figure 2-b), and GCR (Figure 2-c). GPOFA had some spherical particles, as shown in Fig. 1a. Both material particles, GGBFS and GCR, had irregular shapes. However, GGBFS was a solid particle that looked like cement particles, while GCR was apparently a soft particle with a rough surface.

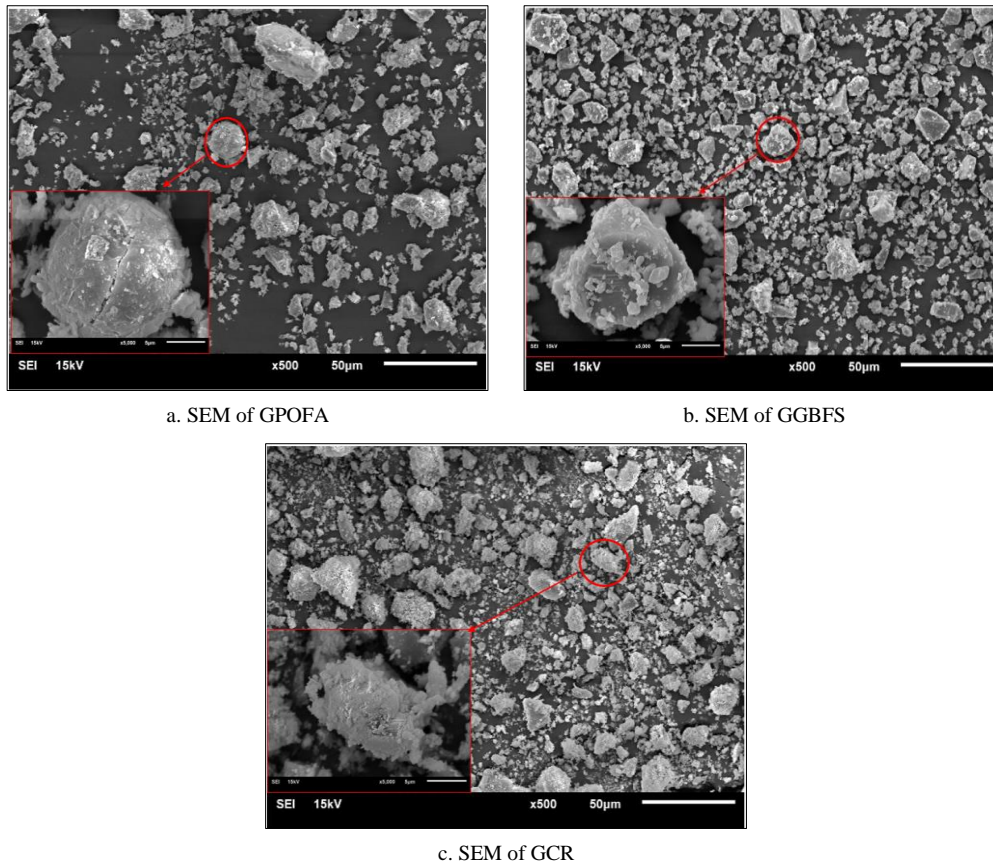


Figure 2. SEM of materials (GPOFA, GGBFS, and GCR)

Table 1 shows the tabulated chemical compositions of GPOFA, GGBFS, and GCR. The sum of silica, alumina, and ferric oxides ($\text{SiO}_2 + \text{Al}_2\text{O}_3 + \text{Fe}_2\text{O}_3$) in GPOFA was more than 50%, and more than 10% CaO was observed in GPOFA. The main component of GGBFS was CaO (38.1%), and in addition, SiO_2 accounted for 36.8%. The total alkali content ($\text{Na}_2\text{O} + 0.658\text{K}_2\text{O}$) and SO_3 content of GGBFS were 0.8% and 1.3%, respectively, which met the chemical requirements for slag cement for use in concrete and mortar according to ASTM C989/C989 [26]. To ensure the reaction properties of GGBFS, the hydration modulus was considered. Chang [27] suggested that the hydration modulus was the ratio of the sum of CaO, MgO, and Al_2O_3 to SiO_2 , which should be not less than 1.4, while the GGBFS used in this study had the hydration modulus of 1.6. GCR consisted of the calcium hydroxide ($\text{Ca}(\text{OH})_2$) and calcium carbonate (CaCO_3) compounds [20, 28–30], thus the CaO of GCR had a high value of 65.40%, and the high LOI of 26.5% was also observed due to the dehydroxylation and decarbonation of GCR during the LOI assay.

Table 1. Chemical compositions of materials

Chemical compositions (%)	GPOFA	GGBFS	GCR
Silicon dioxide (SiO_2)	49.3	36.8	3.9
Aluminum oxide (Al_2O_3)	1.4	14.6	2.3
Ferric oxide (Fe_2O_3)	2.0	0.6	0.5
Calcium oxide (CaO)	15.8	38.1	65.4
Sulfur trioxide (SO_3)	3.9	1.3	0.7
Magnesium oxide (MgO)	3.5	6.5	0.7
Sodium oxide (Na_2O)	0.1	0.3	-
Potassium oxide (K_2O)	13.9	0.8	-
Loss on ignition (LOI)	10.2	1.0	26.5

XRD patterns of raw materials for use as the binders are presented in Figure 3. The broad humps around 20° – 36° 2θ displayed the amorphous phase of the GPOFA. In addition, phases of quartz (SiO_2), corundum (Al_2O_3), dipotassium oxide (K_2O), and lime (CaO) were detected in the GPOFA, which were consistent in chemical composition with x-ray fluorescence (XRF) analysis. GGBFS had a good amorphous phase, while GCR showed mainly phases of portlandite ($\text{Ca}(\text{OH})_2$) and calcite (CaCO_3). For calcite (CaCO_3), it may be formed from the reaction between $\text{Ca}(\text{OH})_2$ of the GCR and carbon dioxide (CO_2) in the air.

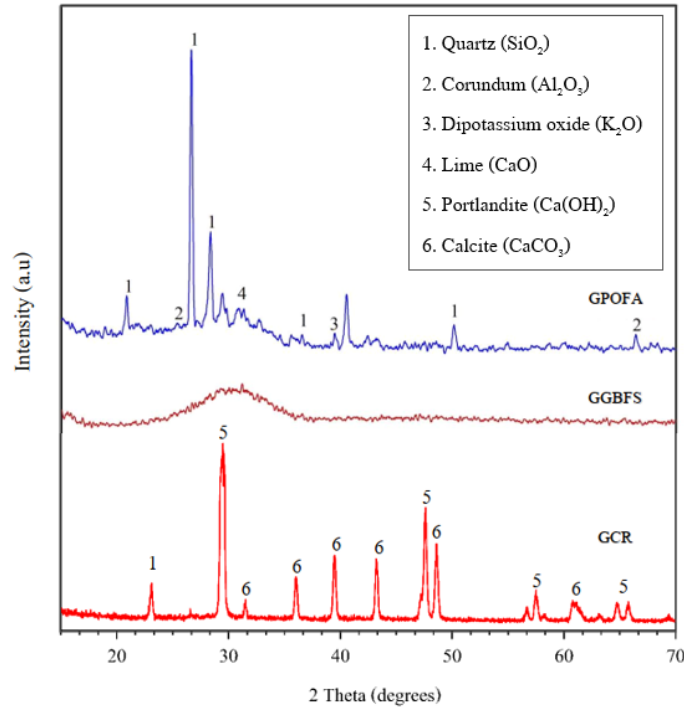


Figure 3. XRD patterns of materials

3. Experimental Design

3.1. Mix Proportion

The method used to determine the volume of each material for the ratio of binary and ternary binders in this study is illustrated in Figure 4. The mortar was divided into 3 groups that contained a high volume of GPOFA (> 50 wt%) in each mortar mixture, as shown in Table 2. In the first group, GPOFA was mixed with GCR; the mixtures of GPOFA:GCR were 85:15, 70:30, and 55:45 wt% (designated as PO85CR15, PO70CR30, and PO55CR45, respectively). The mixtures of GPOFA:GGBFS in wt% were also 85:15 (PO85GB15), 70:30 (PO70GB30), and 55:45 (PO55GB45) for the second groups. The last group was the ternary group consisting of GPOFA:GGBFS:GCR at the ratios 55:15:30, 55:30:15, and 70:15:15 wt% (assigned as PO55GB15CR30, PO55GB30CR15, and PO70GB15CR15, respectively).

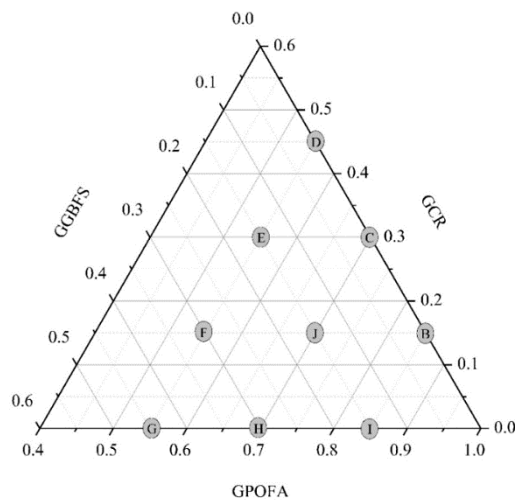


Figure 4. Determination method of the volume of each material (Symbols of B, C, D, I, H, G, E, F and J can be seen in Table 2.)

Table 2. Mix proportion of mortars

Without alkali activator									
Symbols	Mortar	Proportion of materials (wt%)					SP. (wt% of binder)	NaOH (Molar)	Flow (%)
		GPOFA	GGBFS	GCR	Sand	Water			
B	PO85CR15	85	-	15	275	50	1.2	-	108
C	PO70CR30	70	-	30	275	50	2.8	-	106
D	PO55CR45	55	-	45	275	50	3.0	-	105
I	PO85GB15	85	15	-	275	50	1.0	-	111
H	PO70GB30	70	30	-	275	50	1.0	-	112
G	PO55GB45	55	45	-	275	50	1.0	-	107
E	PO55GB15CR30	55	15	30	275	50	1.8	-	108
F	PO55GB30CR15	55	30	15	275	50	1.4	-	105
J	PO70GB15CR15	70	15	15	275	50	1.4	-	107
With alkali activator									
	PO70CR30+N1	70	-	30	275	50	2.0	1	109
	PO70CR30+N2	70	-	30	275	50	3.0	2	108
	PO70GB30+N1	70	30	-	275	50	3.4	1	106
	PO70GB30+N2	70	30	-	275	50	4.2	2	106
	PO55GB30CR15+N1	55	30	15	275	50	3.2	1	107
	PO55GB30CR15+N2	55	30	15	275	50	3.8	2	105

Once the optimum mixture of all 3 groups was obtained, characterized by the highest compressive strength, NaOH flakes were used as an activator at concentrations of 1 and 2 M in each mixing group. The material ratios of the mortar mixes with alkali activator are also shown in Table 2. In this study, the ratio of water to binder (W/B) was constant at 0.5, and the ratio of binder to sand was 1 to 2.75. Superplasticizer polycarboxylate-based (Type A&F) was applied to increase the flowability of the fresh mortar between 105 and 115%. The time frame for mixing the mortar was 8 minutes. In the first 2 minutes, the binder was mixed with 30% water or NaOH solution. Then 40% water or NaOH solution and sand were added and mixed for 3 minutes. Another 30% water or NaOH solution mixed with superplasticizer was added and mixed continuously for 3 minutes to form a homogeneous mortar mixture. For the alkali activated mixture, the NaOH solution was prepared for 24 hours before mixing to reduce the heat of the mixture during mixing. The fresh mortar with mold was wrapped with plastic wrap for 24 hours. After demolding, the mortar sample in each mixture was stored in water under the same conditions to cure.

3.2. Testing Program

3.2.1. Compressive Strength and Weight Change under H₂SO₄ Attack

A 50 mm cubic mortar was used to determine the compressive strength and weight change of the mortar when it was soaked in H₂SO₄ solution. ASTM C109 [31] was used as a guideline for compressive strength testing. A compression rate of 1000 N/s was applied. The compressive strength of the mortar was determined at 7, 28, and 90 days.

To investigate the effect of non-alkali activated mortar compared to alkali activated mortar and the effects of three different binders on the H₂SO₄ attack of the mortar, PO70CR30, PO70GB30, PO55GB15CR30, PO70CR30+N1, PO70GB30+N1, and PO55GB30CR15+N1 mortars were used to determine the change in weight of the mortar. In addition, the groups of the PO55GB30CR15, PO55GB30CR15+N1, and PO55GB30CR15+N2 mortars were tested to study the effects of NaOH concentration. The H₂SO₄ solution was prepared at a concentration of 3 wt% (pH=0.5). Before the mortar samples were soaked in the H₂SO₄ solution, the mortars were cured in water for 28 days to increase their strength. The weight change of the mortar was measured every 1 week until the end of the test at 15 weeks.

For each mortar mixture, the compressive strength and the change in weight of the mortar as a result of the immersion in H₂SO₄ were determined based on the average result of three mortar samples.

3.2.2. Microstructural Analysis

Paste samples of PO70CR30, PO70GB30, PO55GB30CR15, PO70CR30+N1, PO70GB30+N1, PO55GB30CR15+N1, and PO55GB30CR15+N2 (same mix proportion as in Table 2 without sand) were analyzed for microstructure at 28 days by x-ray diffraction (XRD), thermogravimetric analysis (TGA), scanning electron microscopy (SEM), and energy dispersive x-ray spectroscopy (EDS).

XRD was applied to analyze the crystallinity of raw materials and paste samples. The XRD investigation was operated with the diffractometer with x-ray source Cu K α -radiation ($\lambda = 1.5418 \text{ \AA}$) using the scan range from 20 to 70° (2 θ) and resolution of 0.02°/step.

TGA analysis was used to estimate the extent of dehydration, dehydroxylation, and decarbonation of the pastes by examining the mass loss at each temperature range. TGA analysis was performed using a thermogravimetric analyzer (Pyris 1 TGA). The paste sample was heated to 900 °C in a nitrogen gas atmosphere at a heating rate of 10 °C per minute.

The characteristic microstructure, such as the microphotography of the formed hydration, and the chemical elements in each paste sample were analyzed using the techniques of SEM and EDS. Before testing, the paste sample was coated with gold under vacuum conditions to improve electrical conductivity.

4. Results and Discussions

4.1. Compressive Strength of Mortar

4.1.1. Compressive Strength of Mortar without Alkali Activator

Figure 5 presents the contour maps of compressive strength at each mix ratio at 7 days (Figure 5-a), 28 days (Figure 5-b), and 90 days (Figure 5-c). According to these contour maps in Figure 5, a binary binder mixture of GPOFA:GCR shows lower compressive strength of mortar than the binder mixtures of GPOFA:GGBFS. The reaction between GPOFA and GCR is only a pozzolanic reaction, which requires a long time and has a slow reaction rate [17, 20, 32]. Considering that the mortar used the binary binders of GPOFA:GGBFS, the sole GGBFS could generate the hydration products such as C-S-H and Ca(OH)₂ [33, 34]. When GPOFA was used together with GGBFS, the secondary C-S-H was generated from the pozzolanic reaction. Therefore, the compressive strengths of all mortars containing GGBFS in the mixture were higher than those of the mortar made from a binder of GPOFA:GCR. However, in the case of the PO85GB15 mortar, this had a similar compressive strength to those of the GPOFA:GCR mortar due to the PO85GB15 mortar containing a low GGBFS content of 15 wt%. Therefore, the C-S-H from GGBFS hydration occurred to a lesser extent. In addition, the low GGBFS content resulted in a deficiency of Ca(OH)₂ from GGBFS hydration, which affected the pozzolanic reaction with GPOFA.

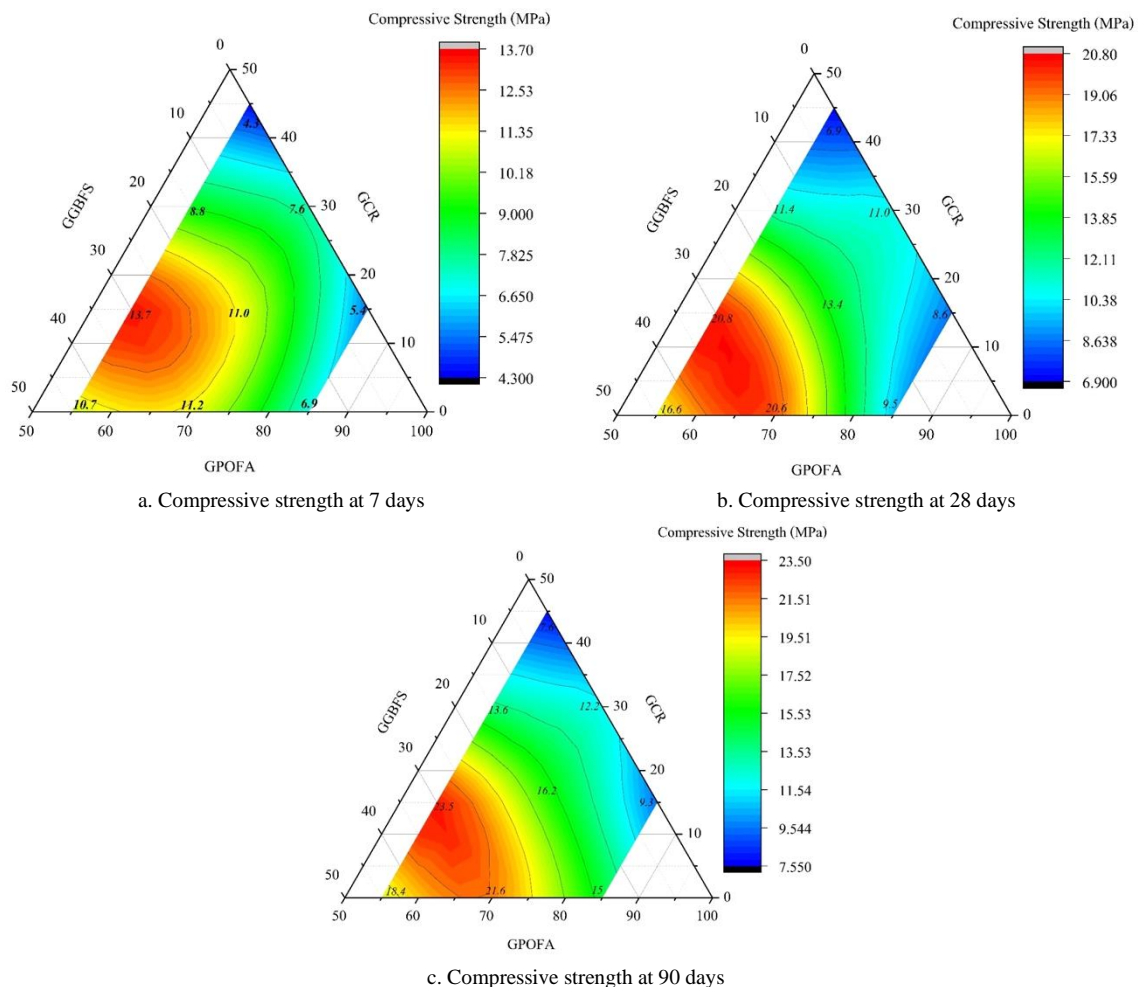


Figure 5. Contour map of mortar compressive strength of different mixtures

To reduce the effect of the lacking $\text{Ca}(\text{OH})_2$, GCR was added to the mixture as a ternary binder. Observation of the compressive strength of PO55GB15CR30 and PO70GB15CR15 mortars (constant GGBFS content of 15 wt%) showed that their compressive strengths were increased comparable to the PO85GB15 mortar, especially at 7 and 28 days. Figure 5-a shows that the compressive strengths of PO55GB15CR30 and PO70GB15CR15 mortars were 8.8 MPa (green color zone) and 11.0 MPa (yellow color zone), while PO85GB15 mortar had a compressive strength of 6.9 MPa (cyan color zone). At 28 days (Figure 5-b), the compressive strengths of PO55GB15CR30 and PO70GB15CR15 mortars were in the green color zone, but the compressive strength of PO85GB15 mortar was still in the cyan color zone. However, the compressive strengths at 90 days of the PO55GB15CR30 and PO70GB15CR15 mortars were as high as those of the PO85GB15 mortar (see Figure 5-c). Furthermore, increasing the GGBFS content to 30 wt% in the ternary binders (PO55GB30CR15 mortar) resulted in the excellent compressive strength of mortar at all curing ages, which was higher than that of the PO70GB30 mortar and all mortar mixtures. This finding indicated that the use of ternary binders consisting of GCR, GPOFA, and GGBFS was more effective in terms of compressive strength than binary binders containing blends of GPOFA with GGBFS and/or GPOFA with GCR. This was due to the fact that the compressive strength could be generated by the products from three reactions, namely the hydration product of GGBFS, the pozzolanic products of GPOFA and $\text{Ca}(\text{OH})_2$ from GCR, and GPOFA and $\text{Ca}(\text{OH})_2$ from the hydration reaction of GGBFS.

From this study, the optimum ratio of the GPOFA:GCR and GPOFA:GGBFS binary binders was for PO70CR30 and PO70GB30. For the ternary binders, the optimum ratio from the mixture of GPOFA:GGBFS:GCR was 55:30:15 wt%.

4.1.2. Compressive Strength of Mortar with the Alkali Activator

For the alkali activated mortar, the PO70CR30, PO70GB30, and PO55GB30CR15 mixtures, each of which exhibited the highest compressive strength for the binary and ternary binders, were used to investigate the effects of NaOH concentration on the compressive strength of mortar. The results of the compressive strengths of the alkali-activated mortars are shown in Table 3. For the mortars with binary binders, the PO70CR30 mortar had compressive strengths of 7.6, 11.0, and 12.2 MPa, and the PO70GB30 mortar had compressive strengths of 11.2, 20.6, and 21.6 MPa at 7, 28, and 90 days, respectively. When 1 M NaOH was added into the mixture, PO70CR30+N1 mortar exhibited the compressive strengths of 10.0, 11.8, and 15.0 MPa at 7, 28, and 90 days, respectively, while the compressive strengths of the PO70GB30+N1 mortar were enhanced to 12.9, 21.5, and 26.3 MPa at 7, 28, and 90 days, respectively. Similarly, the compressive strengths of the ternary binders of the PO55GB30CR15+N1 mortar were higher than those of the PO55GB30CR15 mortar by approximately 0.8, 1.8, and 6.9 MPa at 7, 28, and 90 days, respectively.

Table 3. Compressive strength of mortar with the alkali activator

Mortar	Compressive strength (MPa)		
	7 days	28 days	90 days
PO70CR30	7.6	11.0	12.2
PO70CR30+N1	10.0	11.8	15.0
PO70CR30+N2	3.2	6.1	9.1
PO70GB30	11.2	20.6	21.6
PO70GB30+N1	12.9	21.5	26.3
PO70GB30+N2	8.1	12.4	15.0
PO55GB30CR15	13.7	20.8	23.5
PO55GB30CR15+N1	14.5	22.6	30.4
PO55GB30CR15+N2	8.7	13.2	17.0

According to the experimental findings, the appropriate use of the NaOH concentration herein as 1 M could increase the compressive strength of the mortars made from both binary and ternary binders. This was owing to the silica ion of GPOFA or the silica and alumina ions of GGBFS being leached by NaOH, resulting in a more complete reaction with $\text{Ca}(\text{OH})_2$ [22, 35]. However, the compressive strength of the mortars prepared from all three binders was reduced when 2 M NaOH was added to the mixtures. The higher NaOH concentration affected the workability of the fresh mortar. The mixing process and pouring of the fresh mortar into the mold were difficult because the fresh mortar was very sticky and coagulated quickly. In this case, high air entrapment may occur in the hardening state of the mortar, resulting in lower compaction of the mortar. In addition, there was a possibility that the aluminosilicate gel was precipitated in the initial stages due to the excessive hydroxide ions in the mixture, which led to an impeded subsequent reaction and a decrease in compressive strength [36, 37]. Alonso and Palomo [38] reported that the dissolved ion species (OH^-) increased at the high NaOH concentration, which limited the dispersal of ions and delayed the formation of hardness structures.

For the aforementioned reasons, the mortars in this study with 2 M NaOH had lower compressive strength than the mortars with 1 M NaOH and no NaOH in the mixture. The binary and ternary mortars with the addition of 2M NaOH had compressive strengths ranging from 3.2 to 17.0 MPa, while the binary and ternary mortars with the addition of 1M NaOH and without NaOH addition had compressive strengths ranging from 10.0 to 30.4 and 7.6 to 23.5 MPa, respectively. The diminution in compressive strength owing to the increase in NaOH concentration is consistent with previous studies that investigated the different binders. Najimi et al. [9] discovered that the compressive strength of mortars made from alkali-activated slag mixed with natural pozzolan decreased with the increasing NaOH concentration in the mixture, especially for the mortars with a high content of natural pozzolan and a low content of slag. This was due to the higher NaOH concentration which led to greater difficulties in the diffusion of the ion species in the aqueous phase, resulting in a decrease in the reaction rate. Dueramae et al. [39] summarized that the compressive strength of the mortar containing 70 wt% GFA and 30 wt% GCR as a binder could be increased by adding NaOH at the rate of 0.5–1.0 wt% of the binder. However, when the amount of NaOH was escalated to 2.0 wt% of the binder in the mortar mix, the compressive strength decreased and dropped sharply when NaOH was added in an amount up to 3.0 wt% of the binder.

4.2. Sulfuric Acid (H₂SO₄) Attack

4.2.1. Weight Changes due to H₂SO₄ Attack of Mortar with and without Alkali Activator

The results of the changes in weight owing to a 3% H₂SO₄ solution of non-alkali activated and alkali activated mortar from both binary and ternary binders are presented in Figure 6. The weight changes of the PO70GB30 and PO70GB30+N1 mortars behaved similarly to cement-based mortars in the previous research studies [25, 40]. Most of the spalling on the surface of the mortar was effectuated by the combination of decalcification and dealumination of C-S-H and C-A-S-H at the surface, rather than by internal expansion of the mortar. This weight loss phenomenon also occurred in alkali-activated concrete made from GGBFS as a binder in the previous study [41].

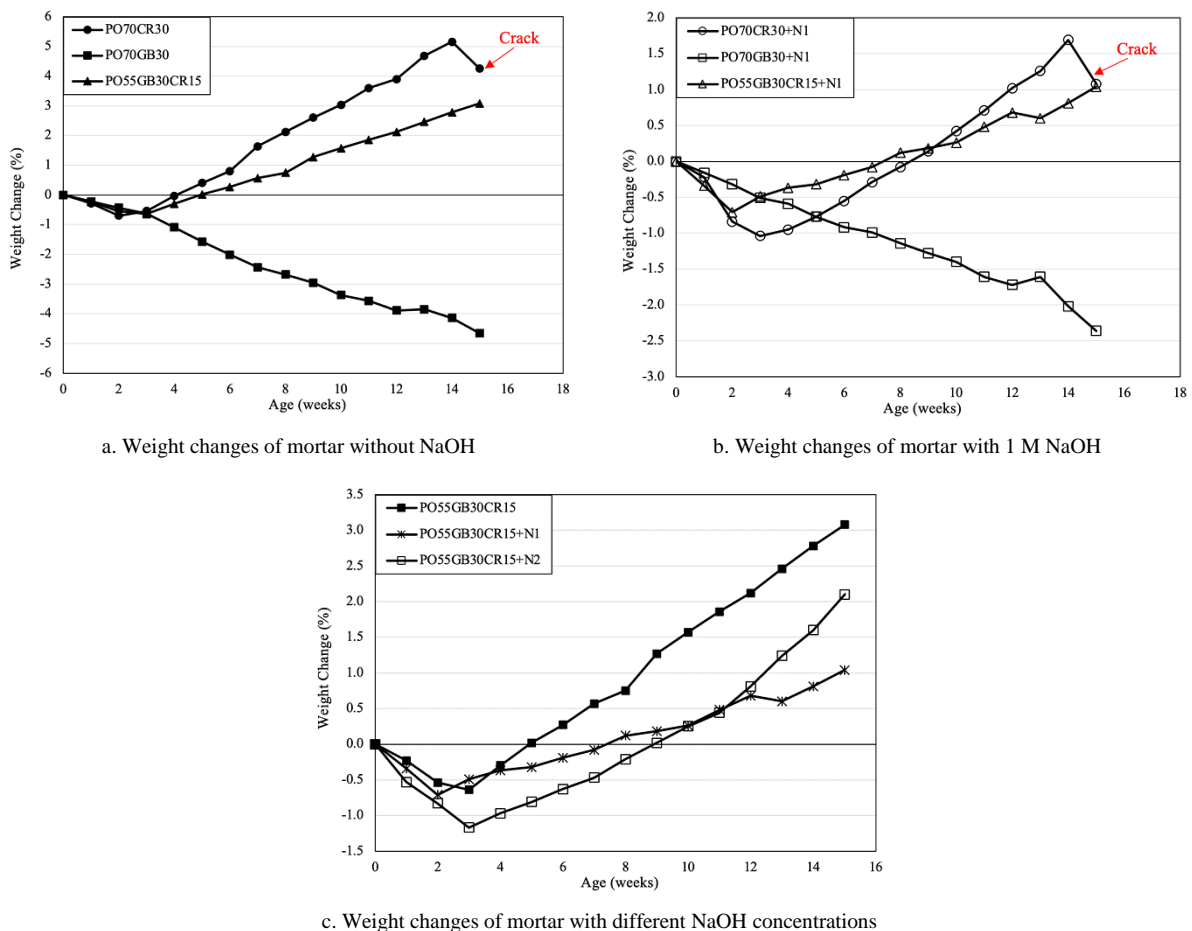


Figure 6. Weight changes due to H₂SO₄ attack of mortar

The weight of the PO70GB30 mortar decreased continuously with the increasing duration of immersion. At 15 weeks of immersion, the weight loss was 4.66% (Figure 6-a). The PO70GB30+N1 mortar (Figure 6-b) also showed a continuous weight loss, but the final weight loss of the PO70GB30+N1 mortar was 2.36%, which was lower than that of the PO70GB30 mortar. The PO70GB30+N1 mortar could reduce the weight change by up to 49% as compared to

PO70GB30 without NaOH activation. This was due to the fact that the PO70GB30+N1 mortar exhibited higher compressive strength than the PO70GB30 mortar, indicating the higher density of the mortar. In addition, according to EDS results (Section 4.3.3.), PO70GB30 paste had a higher calcium content than the PO70GB30+N1 paste. Therefore, more calcium ions (Ca^{2+}) resulted in the greater ion exchange of calcium ions with acid protons such as H^+ and H_3O^+ or greater formation of calcium sulfate (gypsum) by the reaction of calcium ions with sulfate ions (SO_4^{2-}), resulting in greater decomposition of the structure of the hardened product [42, 43]. Although sodium ions in the PO70GB30+N1 mortar could also be leached by an electrophilic attack with acidic protons, PO70GB30+N1 mortar contained much less sodium ions compared to calcium ions. Moreover, sodium ions were leached to a considerably lower extent than calcium ions for the process of corrosion by acid [44]. The weight change of the PO70GB30 and PO70GB30+N1 mortars showed that the emergence of calcium sulfate was confined to the surface of the mortar, with no or less propagation to the inner part of the mortar.

However, the behavior of the weight change of the mortar containing GCR in the mixtures (PO70CR30, PO55GB30CR15, PO70CR30+N1 and PO55GB30CR15+N1 mortars) was different from those of the PO70GB30 and PO70GB30+N1 mortars. The weight of the mortar decreased only in the first 3-4 weeks, and thereafter the weight of the mortar tended to increase continuously. The highest weight gain of 5.16 and 1.69% was observed at 14 weeks in the PO70CR30 and PO70CR30+N1 mortars, respectively, and then the sample was cracked at 15 weeks, as shown in Figure 7. For the PO55GB30CR15 and PO55GB30CR15+N1 mortars, the weight of the mortars after immersion for 15 weeks increased to 3.08 and 1.04%, respectively. This finding suggested that the weight loss in the first 3-4 weeks indicates an attack of H_2SO_4 on the surface of the mortar. As the acidic solution migrated into the mortar, the H_2SO_4 reacted with the calcium component, especially the $\text{Ca}(\text{OH})_2$, which occurred at high levels in the mortar containing GCR in the mixture. The increase in weight of these mortars could be due to calcium sulfate inside the mortar matrix which formed by the reaction of calcium ions with sulfate ions. In the initial stage, calcium sulfate filled the pores and shrinkage microcracks [44]. Note that the PO70CR30 mortar had the change in weight decreased of 62% with adding of 1M NaOH similar to the change in weight of PO55GB30CR15 mortar was also reduced up to 66% with adding of 1M NaOH. Thus, the addition of 1M NaOH as alkali activator could reduce the change in weight both of binary binder of GPOFA-GCR and ternary binder of GPOFA-GGBS-GCR. In the other the 1M of NaOH activator was significantly affected to improve acid resistance.

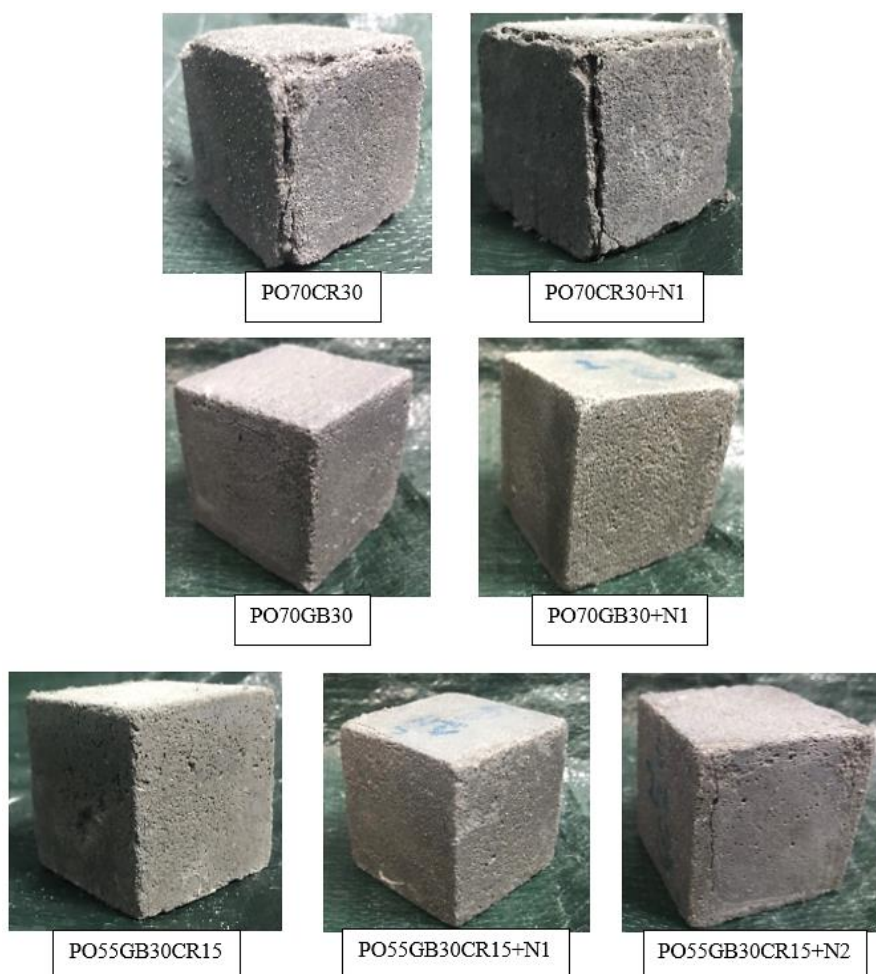


Figure 7. Surface appearance of mortar after 15 weeks immersion in sulfuric acid

When sufficient calcium ions were present in the system, continuous deposition of calcium sulfate occurred over a long period of time, resulting in an increase in the weight of the mortar. However, this continuous deposition of calcium sulfate in the low strength mortar led to expansion and internal stresses which resulted in cracks in the corners, as observed in the PO70CR30 and PO70CR30+N1 mortars (clearly visible in Figure 7). This analogous mechanism of the H_2SO_4 solution destruction was found in alkali activated GGBFS mortar incorporation with hydrated lime [25]. That is, there was an ion exchange between the calcium ions and the cations of the acid on the surface, which led to a disruption of the silicate framework on the surface during the first period. When the acidic solution was allowed to penetrate the mortar, it caused calcium sulfate to accumulate until the mortar expanded and eventually cracked. Moreover, the binary binder from GPOFA and GGBBF showed better performance than the binary binder from GPOFA and GCR when exposed to H_2SO_4 solution due to difference in chemical and phase compositions. The different behavior between the mixture with and without GCR could also be explained by the fact that $Ca(OH)_2$ in GCR readily adsorbs the H_2SO_4 solution, leading to the immediate formation of the calcium sulfate in the first reaction. In the PO70GB30 and PO70GB30+N1 mortars (without GCR), the $Ca(OH)_2$ was formed by the hydration reaction of GGBFS, which was accompanied by the formation of C-S-H. Therefore, the calcium sulfate in the PO70GB30 and PO70GB30+N1 mortars was formed by a secondary reaction and may occur along with the formation of the pozzolanic product derived from the reaction between GPOFA and $Ca(OH)_2$ from the hydration reaction of GGBFS. It is possible that the erosion of the mortar without GCR is due to the gradual destruction of the solid structure such as C-S-H and C-A-S-H (as described above) greater than the accumulation of calcium sulfate in the mortar. In comparison to alkali activated slag (AAS) [41], in which NaOH and Na_2SiO_3 were used as alkali activators, the AAS mortar exhibited a lower weight loss than the PO70GB30 and PO70GB30+N1 mortars. At 13 weeks, the weight losses of the PO70GB30 and PO70GB30+N1 mortars were -4% and -1.7%, respectively, while the AAS mortar demonstrated a weight loss between -0.5% and -1.7%, depending on the NaOH molarity and the NaOH/ Na_2SiO_3 ratio. It is noteworthy that the strengths of PO70GB30 and PO70GB30+N1 mortars were inferior to those of AAS mortars.

4.2.2. Effect of NaOH Dosage on Weight Changes due to H_2SO_4 Attack

The investigation of the change in weight of the mortar at different NaOH dosages on the mixture of ternary binders is shown in Figure 6-c. Since the ternary binder mortar contained GCR in the mixture, the weight of the mortar increased during the 15 weeks of soaking in H_2SO_4 , which was explained in the above section. The weight gains of the PO55GB30CR15, PO55GB30CR15+N1 and PO55GB30CR15+N2 mortars were 3.08, 1.04 and 2.10%, respectively. The result showed that the use of NaOH as an alkali activator could reduce weight gain. This was explained by the fact that the use of NaOH could accelerate the reaction of GGBFS and the reaction between $Ca(OH)_2$ and SiO_2 [45], which probably resulted in a lower $Ca(OH)_2$ content in the PO55GB30CR15+N1 and PO55GB30CR15+N2 mortars. Meanwhile, the PO55GB30CR15 mortar contained more $Ca(OH)_2$ due to the non-accelerated reaction with NaOH (see TGA results), therefore, the interaction between $Ca(OH)_2$ and H_2SO_4 was rapid and the deposition of calcium sulfate was much higher. It should be noted that the PO55GB30CR15+N2 mortar had a lower weight gain than PO55GB30CR15 mortar, but the visual observations for PO55GB30CR15+N2 mortar appear to reveal initially cracking at the corner. This was attributed to the higher concentrations of NaOH in PO55GB30CR15+N2 mortar which promoted the rapid formation of the products of hydration of GGBFS and the pozzolanic reaction, resulting in rough surfaces and uneven distribution, thus forming a defective structure and lower strength [46]. Teymouri et al. [41] was also found that excessively high concentrations of NaOH in alkali activated slag mixture causes more irregular structures and high pore structure contents in the microstructure matrix led to negatively affected after exposed to acid. Therefore, even though the deposition of calcium sulfate in PO55GB30CR15+N2 mortar was not as high as in PO55GB30CR15 mortar (which can be observed as a weight increase), the internal stress in the low strength mortar could lead to mortar cracking.

4.3. Microstructural Analysis

4.3.1. XRD

Figure 8 illustrates the XRD patterns of the pastes in this study. For three binders without alkali activator (Figure 8-a), the XRD patterns of PO70CR30, PO70GB30 and PO55GB30CR15 pastes showed the product of C-S-H (tobermorite) which had the hump position at $29.5^\circ 2\theta$. This result proved that GCR and GPOFA could be used as cementing materials via the pozzolanic reaction between portlandite in GCR and oxides of silica in GPOFA. Figure 8-a gives further information that the aluminosilicate (Al_2O_5Si) phase was detected in the form of kyanite, andalusite, and sillimanite. Moreover, calcium aluminosilicate ($CaAlSiO_4$) appeared in the PO55GB30CR15 paste. This was attributed to the fact that the supplementation of GCR in a binder caused an increase in calcium ions in the system. Since the binder was rich in calcium while GGBFS contained alumina ions, the C-S-H in the system could be synthesized or replaced to stabilize the C-A-S-H [47, 48].

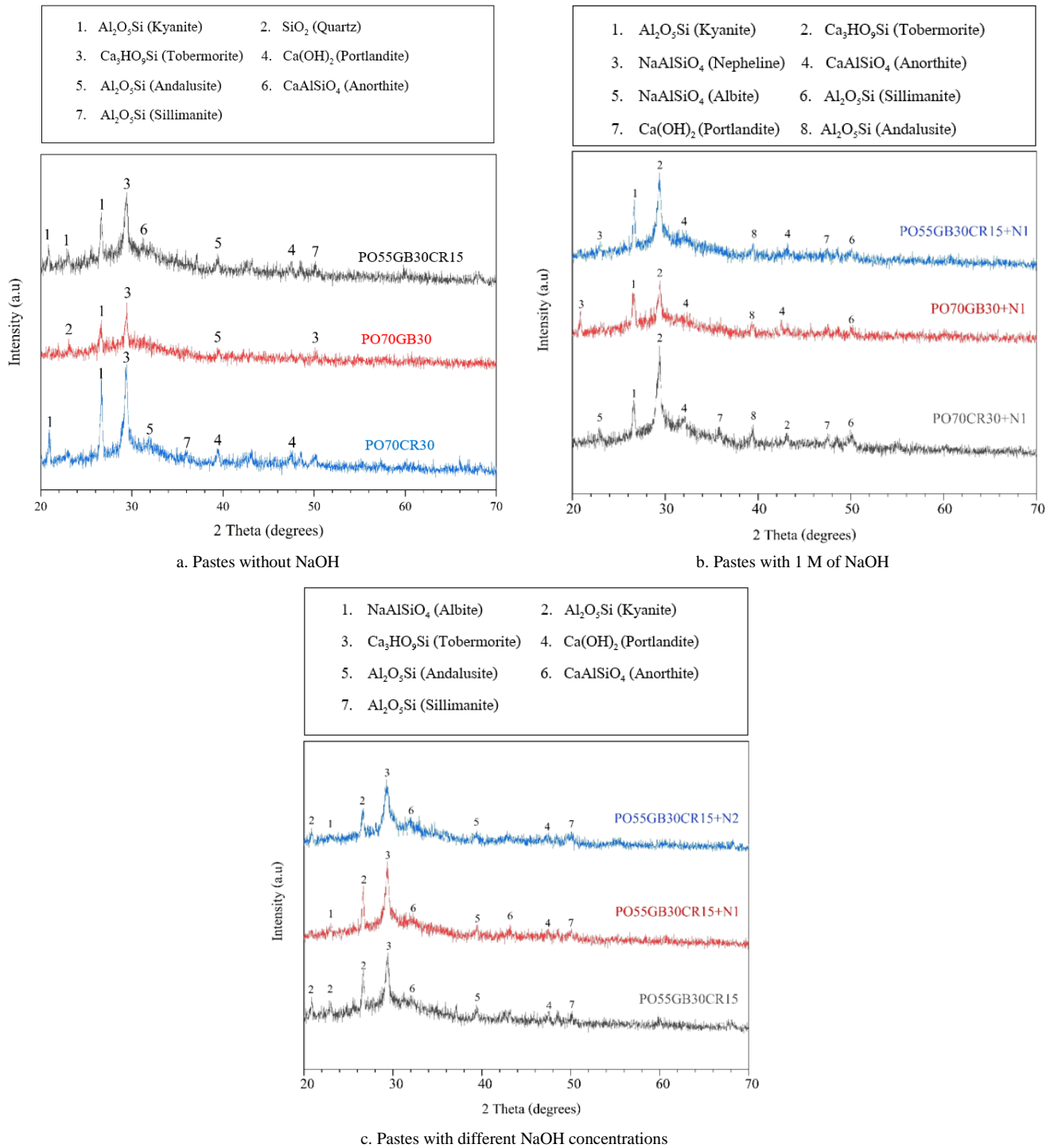


Figure 8. XRD patterns of pastes

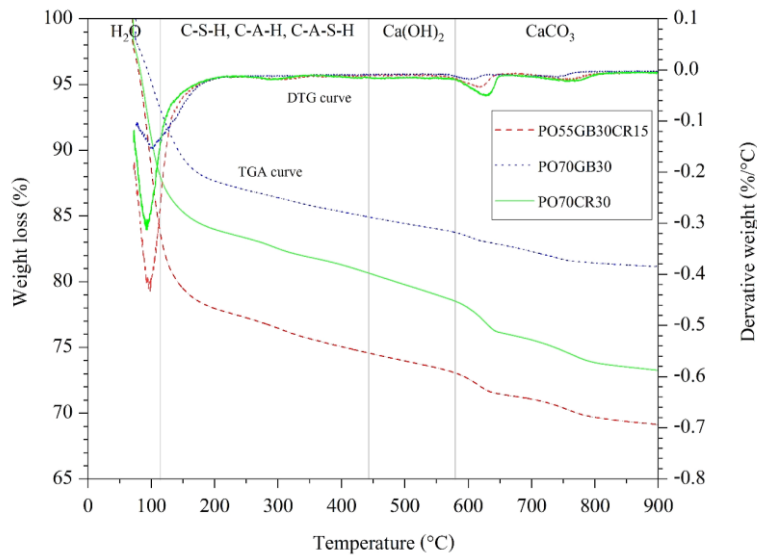
The XRD patterns of the pastes with different binders with 1 M NaOH (Figure 8-b) also showed C-S-H. However, sodium aluminosilicate (NaAlSiO₄) was detected in the form of albite and nepheline. It should be noted that the PO70CR30+N1 and PO70GB30+N1 pastes contained calcium aluminosilicate, while the PO70CR30 and PO70GB30 pastes did not appear. The presence of calcium in the alkali activated paste system could be replaced by sodium and aluminum, resulting in C-A-S-H, sodium aluminosilicate hydrate (N-A-S-H), or a hybrid C-(N)-A-S-H [20, 48]. The apparent C-A-S-H in the alkali-activated binder may result in greater compressive strength of the mortar than is the case with the non-alkali-activated binder.

Figure 8-c displays the effects of NaOH in the mixtures. The paste sample without NaOH appeared to have lower peak intensity at 29.5° and 32.5° 2θ than the paste sample with NaOH in the mixture. It was possible that the presence of NaOH in the mixture enhanced the pH of the pore solution, leading to an increased occurrence of C-S-H and C-A-S-H [49]. Considering the mixture with 1 M NaOH (PO55GB30CR15+N1 paste) and 2 M NaOH (PO55GB30CR15+N2 paste), the peak of C-S-H at 29.5° 2θ of the PO55GB30CR15+N1 paste was sharper than that of the PO55GB30CR15+N2 paste, indicating the growth of strength [50]. The result of the XRD investigation also showed that the peaks of both the calcium silicate and aluminosilicate products were higher in the mixture with 1 M NaOH than

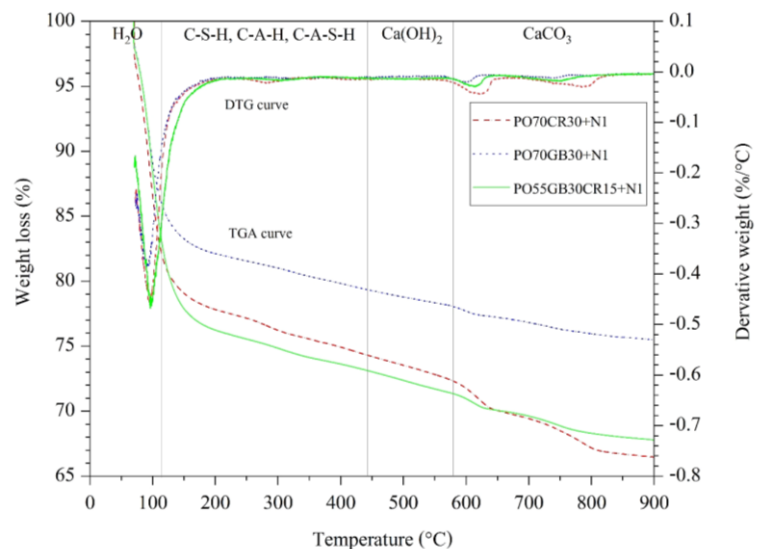
in the mixture without NaOH. However, when the NaOH concentration was increased to 2 M, it was clearly seen that the peak of those products was lower than that of the mixture with 1 M NaOH and even lower than that of the mixture without NaOH addition. This result was confirmed by the compressive strength result, which explains the effect of NaOH concentration on the compressive strength. Furthermore, it was observed in Figures 8-a to 8-c that the XRD patterns of pastes containing GCR exhibited $\text{Ca}(\text{OH})_2$. This was the reason that the mortars with GCR in the mixture showed a significant increase in weight when the mortars were exposed to H_2SO_4 . Certainly, $\text{Ca}(\text{OH})_2$ can easily react with H_2SO_4 to form calcium sulfate, as described above.

4.3.2. Thermogravimetric Analysis

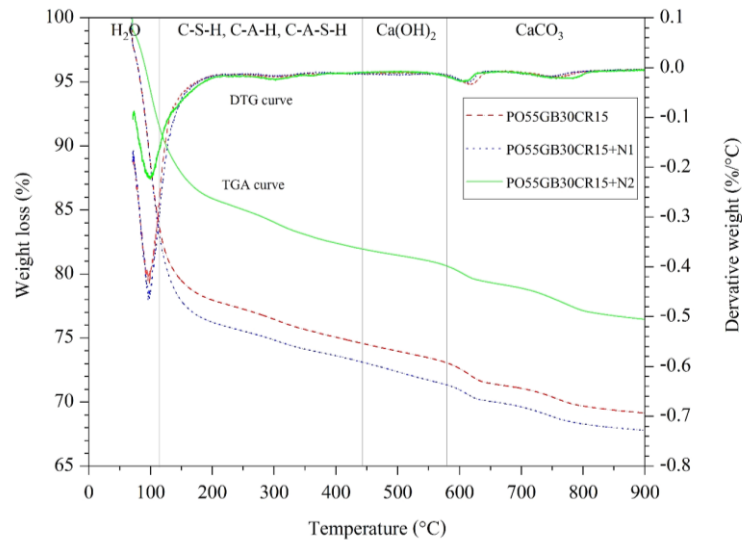
The evaluation of thermogravimetric analysis (TGA) and derivative thermogravimetric (DTG) of the paste with and without alkali-activated pastes is illustrated in Figures 9-a to 9-c. It could be seen that the TGA/DTG curves showed a very rapid mass loss that occurred in the large cusps of the peak temperature of nearly 100 °C, especially for the pastes containing GCR in the mixture. This spectacle was attributed to the fact that the pastes with GCR in the mixture contained more calcium ions, which could store the pore water rather than the paste without GCR in the mixture [51, 52]. Therefore, the free water was more easily evaporated, resulting in an increase in the mass loss at temperatures below 100 °C. Figures 9-a to 9-c give further information that the little cusps of the DTG curve in the pastes containing GCR occur after temperatures higher than 550 °C. This means that decarbonation had occurred. GCR consisted mainly of $\text{Ca}(\text{OH})_2$ and CaCO_3 as shown in Figure 3. It is the fact that at suitable humidity, $\text{Ca}(\text{OH})_2$ can react with CO_2 in the air to form CaCO_3 . Moreover, it was noteworthy that for samples without an alkali activator (Figure 9-a), the final mass loss at a temperature of 900 °C tended to decrease significantly when the samples contained a higher amount of GPOFA. It was possible that the samples without an alkali activator led to a decrease in the reaction rate and consequently to high amounts of unreacted GPOFA. Therefore, the amorphous silica of GPOFA can be transformed into the crystallization of cristobalite and quartz at a temperature of up to 900 °C [53].



a. Pastes without NaOH



b. Pastes with 1 M of NaOH



c. Pastes with different NaOH concentrations

Figure 9. TGA and DTG curves of pastes

For the products of hydration, these could be determined by mass loss in thermal analysis. However, it was not possible to determine the quantity of each hydration product because there was overlap in each temperature range [54]. Thus, in this study, the temperature was separated into three ranges to determine the distinction in products from the changes in mass loss. The mass changes in the temperature ranges of 105–440 °C involved dehydration such as C-S-H and C-A-S-H phases. Dehydroxylation ($\text{Ca}(\text{OH})_2$) and decarbonation (CaCO_3) occurred in the temperature ranges of 440–580 °C and 580–900 °C, respectively [55–57], as shown in Table 4. The symbols ΔM_1 , ΔM_2 , and ΔM_3 represent the percentage changes in mass loss at the temperature ranges of 105–440 °C, 440–580 °C, and 580–900 °C, respectively.

Table 4. Calculation of mass changes from TGA curve

Pastes	Dehydration (105-440 °C)	Dehydroxylation (440-580 °C)	Decarbonation (580-900 °C)
	ΔM_1 (%)	ΔM_2 (%)	ΔM_3 (%)
PO70CR30	8.95	2.22	5.25
PO70GB30	9.48	1.20	2.60
PO55GB30CR15	12.01	1.82	3.91
PO70CR30+N1	10.32	2.04	5.84
PO70GB30+N1	11.10	1.33	2.56
PO55GB30CR15+N1	13.18	1.55	3.55
PO55GB30CR15+N2	11.23	1.36	4.15

Considering the dehydration of the samples without the alkali activator, ΔM_1 was 8.99, 9.48, and 12.01% for the PO70CR30, PO70GB30, and PO55GB30CR15 pastes, respectively. According to these results, the appearance of the hydration products of the binary binders of PO70CR30 was lower than for PO70GB30. Since GGBFS is a good amorphous material (see Figure 3), this has led to the fact that GGBFS generates the hydration products itself upon contact with water and can also react with GPOFA through a pozzolanic reaction. However, the ternary binders with a GCR content of 15 wt% in the mixture was able to promote the hydration products because $\text{Ca}(\text{OH})_2$ in the GCR facilitated a more complete pozzolanic reaction. Guo et al. [58] observed that the pozzolanic reaction of GGBFS was accelerated when the alkaline component $\text{Ca}(\text{OH})_2$ was added to the system, resulting in greater formation of hydration products. The alkali activated pastes with a concentration of 1 M NaOH for the PO70CR30+N1, PO70GB30+N1, and PO55GB30CR15+N1 pastes had ΔM_1 of 10.32, 11.10 and 13.18%, respectively.

Comparing the content of hydration products between the pastes without and with NaOH in the mixtures, the pastes with a concentration of 1 M NaOH were overall more enriched in hydration products than the pastes without NaOH. As mentioned earlier, the leached silica and alumina oxides by NaOH led to enhancements in dissolved silicates and aluminates resulting in the increased reaction with $\text{Ca}(\text{OH})_2$. Thermogravimetric analysis also found that the pastes with GCR in the mixture had a higher percentage of dehydroxylation than the mixture without GCR. This may be attributed to the unreacted GCR in the mixture, which led to the decomposition of $\text{Ca}(\text{OH})_2$ from the components of the raw GCR at elevated temperatures. Thus, the TGA result of the mixture with GCR had a higher weight loss at the temperature of

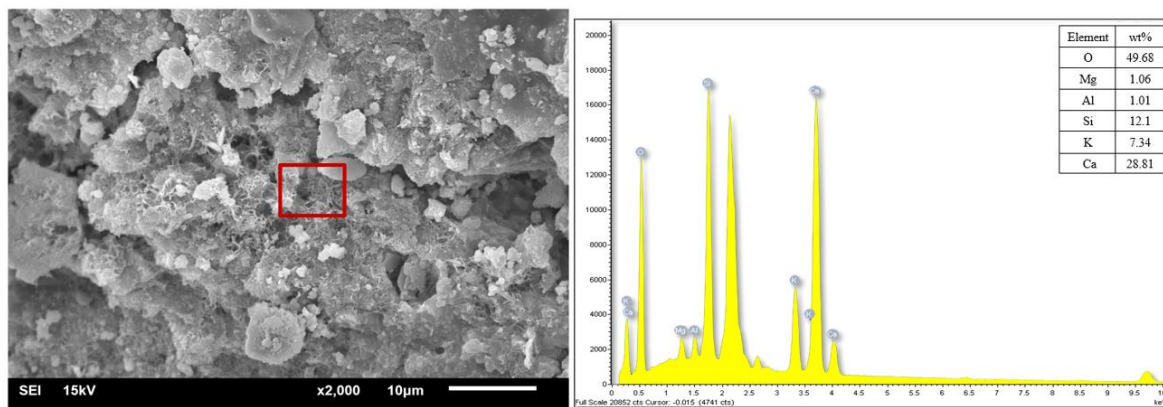
dehydroxylation and decarbonation than the mixture without GCR. This result was related to the XRD analysis. Moreover, the percentage of decarbonation of the pastes had a high value, especially for the PO70CR30 and PO70CR30+N1 pastes, for which the reasons had been discussed above.

The PO55GB30CR15, PO55GB30CR15+N1, and PO55GB30CR15+N2 pastes were used to explain the effects of different NaOH concentrations. $\Delta M1$ was 12.01, 13.18 and 11.23% for the PO55GB30CR15, PO55GB30CR15+N1, and PO55GB30CR15+N2 pastes, respectively. It was noteworthy that the percentage of dehydration of these pastes significantly correlated with their compressive strength of the mortar. However, the PO55GB30CR15+N2 paste had a higher percentage of dehydration than the PO70GB30 paste and a similar value to the PO70GB30+N1 paste while the compressive strength of the PO55GB30CR15+N2 mortar was lower than that of the PO70GB30 and PO70GB30+N1 mortars. It was possible that the PO55GB30CR15+N2 mortar developed more hydration products, but these hydration products were present in the form of a poor pore structure due to the high NaOH concentration in the mixture [46].

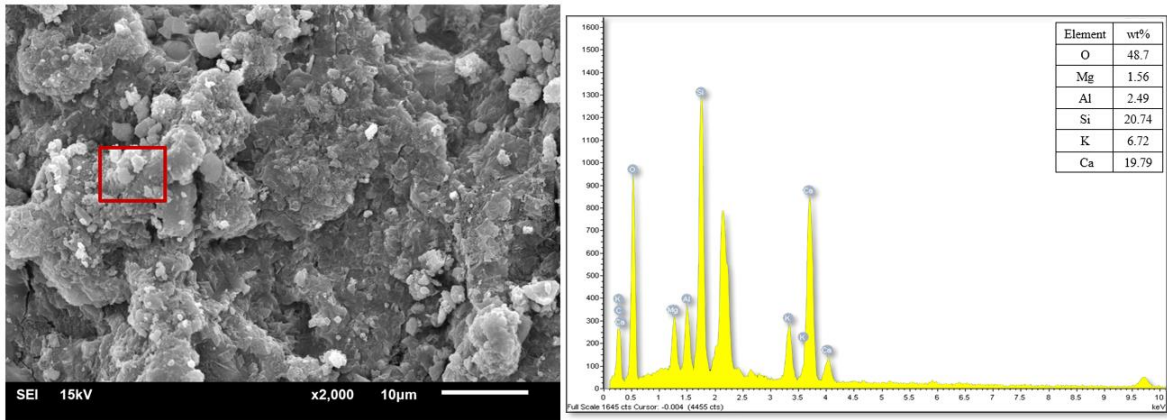
4.3.3. SEM/EDS

Figure 10 exhibits SEM/EDS of the pastes from the binary and ternary binders. According to the SEM microphotographs, the pastes without NaOH (Figures 10-a to 10-c) showed the unreacted raw materials. More pores and irregular structures were observed. Meanwhile, the SEM microphotographs of pastes with a concentration of 1 M NaOH (Figures 10-d to 10-f) illustrated fewer pores and denser structures compared with the pastes without NaOH. This finding confirms that the use of NaOH as an accelerator was able to improve the microstructure of the pastes prepared from binary binders (PO70CR30 and PO70GB30) and ternary binders (PO55GB30CR15). Thus, the mortar with a concentration of 1 M NaOH gave better results in compressive strength and H_2SO_4 attack than the mortar without NaOH in the mixture. The visual observations on SEM microphotograph of the PO70CR30+N1 paste (Figure 10-d) showed a rough and irregular surface in the structural matrix compared with the PO70GB30 and PO55GB30CR15 pastes, which corresponded to the compressive strength; i.e., the compressive strength of the PO70CR30+N1 mortar was much lower than that of the PO70GB30 and PO55GB30CR15 mortars. Additionally, the structure of the paste with a rough and irregular surface could be easily leached out when exposed to an acidic environment [41]. The SEM microphotograph of the PO55GB30CR15+N2 paste (Figure 10-g) showed the paste at a high NaOH concentration. It showed more pores and unevenly distributed surfaces. Fu et al. [46] reasoned that although the formation of hydration products was rapid at a high NaOH concentration, the formation pattern had poor pores in the microstructure of the paste.

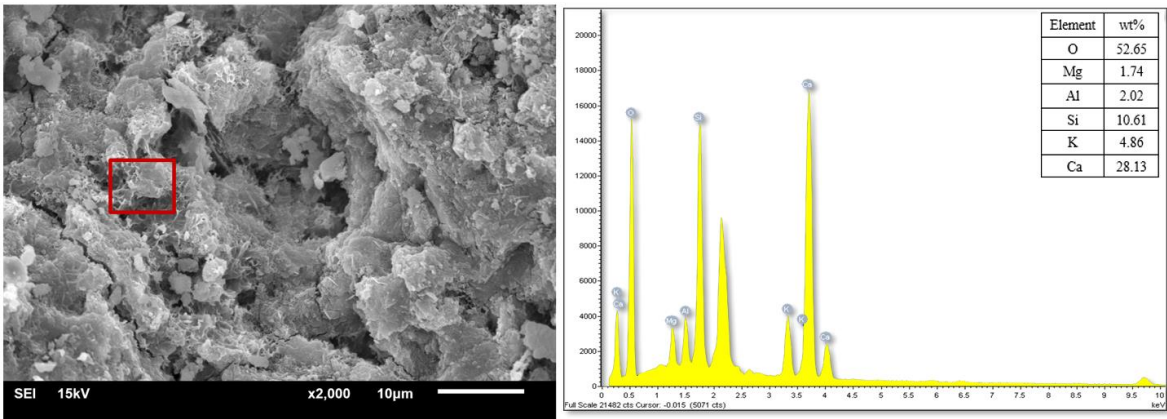
The EDS results of both the binary and ternary pastes showed the major elements of Ca and Si, indicating the C-S-H formation consistent with the XRD information. It should be noted that the pastes containing GCR in the mixtures indicated a higher element of Ca than the pastes without GCR. This suggests that the Ca element not only comes from the formation of hydration products, but that the Ca element could also come from unreacted $Ca(OH)_2$ from GCR, especially the PO70CR30 paste. Obviously, the apparently high content of this Ca element in the pastes had a significant influence on the weight increase of the mortar when immersed in H_2SO_4 solution. Moreover, the K element was present in all pastes because these pastes contained the high-volume GPOFA, which had high K_2O content. Certainly, the pastes with 1 M NaOH (Figures 10-d to 10-f) appeared as Na elements. With the number of Na, O, Al, Si and Ca elements, N-A-S-H or C-(N)-A-S-H products could be formed [59]. When the EDS results were examined together with the XRD results of the pastes with 1 M NaOH, it was possible that C-A-S-H products could be formed because the addition of NaOH to the mixtures increased the pH, which increased the number of C-A-S-H products [49]. For the PO55GB30CR15+2N paste, the result of EDS was not different from that of the PO55GB30CR15+1N paste. However, as described above, the characteristic structure of the PO55GB30CR15+1N paste seemed to be better than that of the PO55GB30CR15+2N paste, describing a good compressive strength and higher H_2SO_4 resistance of the PO55GB30CR15+1N mortar.



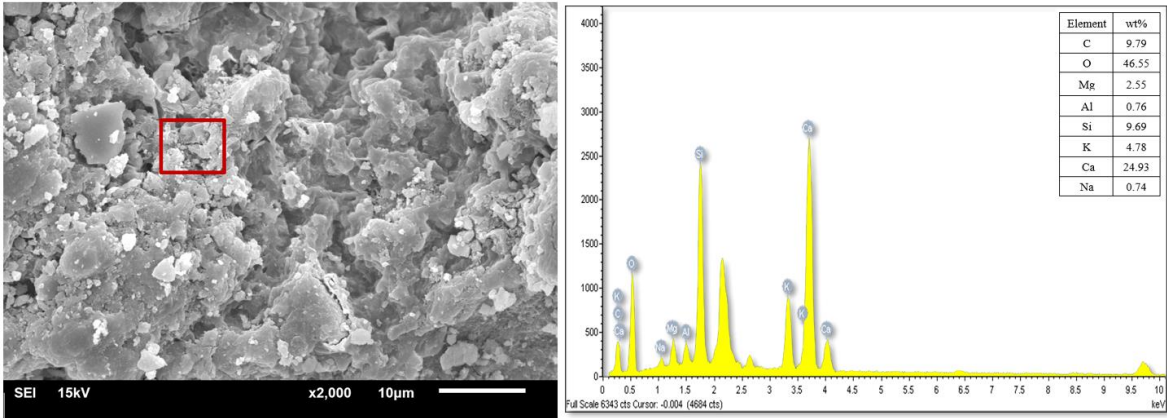
10a. PO70CR30 paste



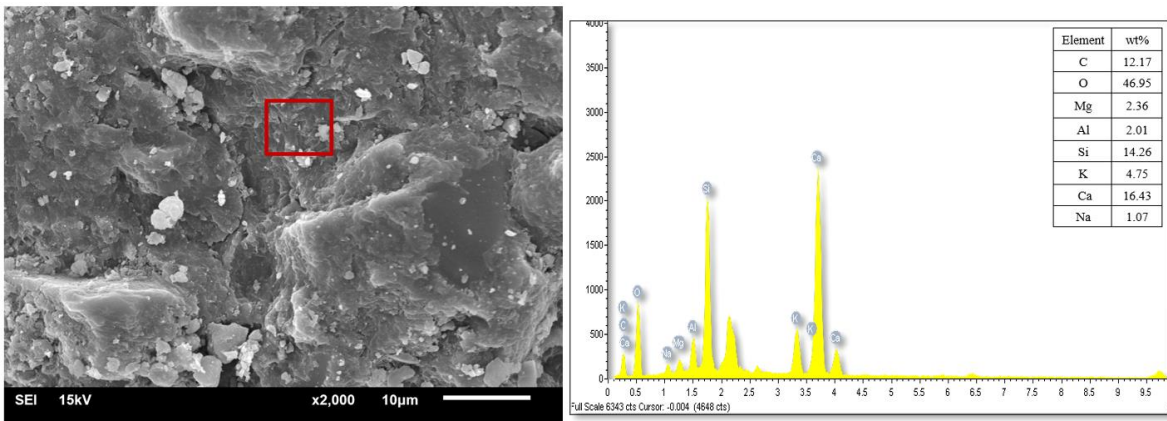
10b. PO70GB30 paste



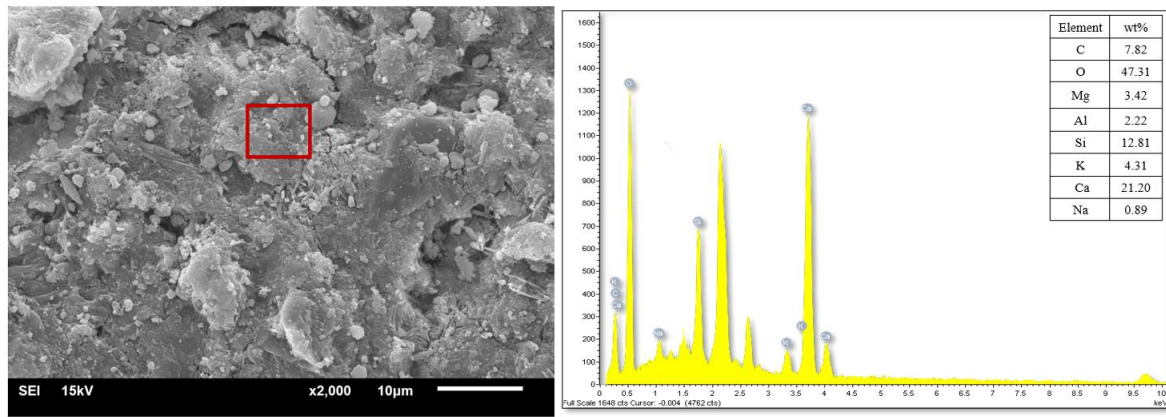
10c. PO55GB30CR15 paste



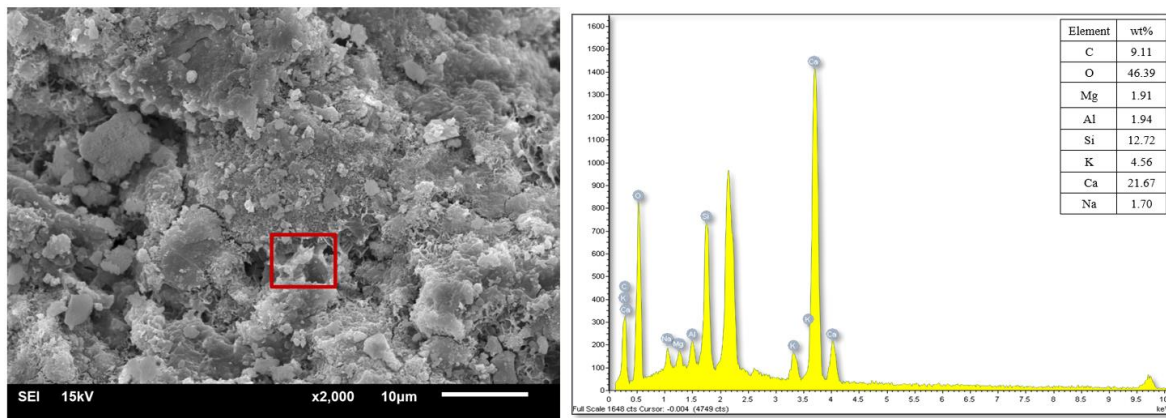
10d. PO70CR30+N1 paste



10e. PO70GB30+N1 paste



10f. PO55GB30CR15+N1 paste



10g. PO55GB30CR15+N2 paste

Figure 10. SEM and EDS of pastes

5. Conclusions

This study contributes to the development of the waste materials from POFA, GGBFS, and CCR as the binder. The investigation of mortars and pastes with and without the alkali activator made of binary and ternary binders on compressive strength, H_2SO_4 attack, and microstructure analysis is summarized as follows:

- In this study, optimal binder ratios were determined for both binary and ternary mixtures. The binary binders GPOFA:GCR and GPOFA:GGBFS in a ratio of 70:30 wt% achieved the highest compressive strengths of 12.2 MPa and 21.6 MPa at 90 days for the PO70CR30 and PO70GB30 mortars, respectively. Notably, the ternary binder GPOFA:GGBFS:GCR in a ratio of 55:30:15 wt.% (PO55GB30CR15) yielded the highest overall compressive strength of 23.6 MPa at 90 days.
- The use of 1 M NaOH as an alkali activator significantly accelerated the compressive strength development in both binary and ternary mortars. However, formation of hydration products was rapid at a concentration of 2 M NaOH, which exhibited a detrimental effect on the compressive strength of the mortar.
- The mortar prepared from PO70GB30 as a binder exhibited weight loss with increasing duration of immersion in a 3% H_2SO_4 solution. This behavior was in contrast to the mortar with GCR in the mixture, which increased in weight at the end of the immersion time. In particular, a high proportion of CCR in the mixture (PO70CR30 mortar) showed low resistance in the H_2SO_4 environment and cracked after 14 weeks of immersion.
- Both binary and ternary mortars containing NaOH showed less weight change when immersed in a 3% H_2SO_4 solution. This indicates that the addition of NaOH as an alkali activator increases the resistance of the mortar to H_2SO_4 environments.

The XRD and EDS analyses showed C-S-H as the primary component of the pastes. In addition, the alkali-activated pastes displayed the presence of N-A-S-H and C-A-S-H phases. The TGA results indicated a higher mass loss of hydration products in alkali-activated pastes compared to non-alkali-activated pastes, which correlated with their higher compressive strength. Correspondingly, SEM observations revealed denser microstructures in alkali-activated pastes compared to non-alkali-activated pastes. However, the use of a higher NaOH concentration at 2 M resulted in a poorer microstructure than the paste with 1 M NaOH.

6. Declarations

6.1. Author Contributions

Conceptualization, W.T. and A.A.; methodology, N.S., A.A., and W.T; validation, S.H., W.T., and C.J.; formal analysis, A.A. and S.D.; investigation, A.A.; resources, N.S.; data curation, A.A.; writing—original draft preparation, A.A. and S.D.; writing—review and editing, S.H., W.T., and C.J.; visualization, A.A.; supervision, W.T. and C.J.; project administration, A.A.; funding acquisition, A.A. All authors have read and agreed to the published version of the manuscript.

6.2. Data Availability Statement

The data presented in this study are available on request from the corresponding author.

6.3. Funding

This study was funded by the Office of the Permanent Secretary, Ministry of Higher Education, Science, Research and Innovation Grant No. RGNS 63-129.

6.4. Acknowledgements

The authors gratefully acknowledge financial support from the Office of the Permanent Secretary, Ministry of Higher Education, Science, Research and Innovation Grant No. RGNS 63-129. Thanks are also extended to the Thailand Science Research and Innovation (TSRI) Basic Research Fund: Fiscal year 2024 under project Advanced and Sustainable Construction Towards Thailand 4.0.

6.5. Conflicts of Interest

The authors declare no conflict of interest.

7. References

- [1] Santos, M. M., Marques Sierra, A. L., Amado-Fierro, Á., Suárez, M., Blanco, F., La Fuente, J. M. G., Diez, M. A., & Centeno, T. A. (2023). Reducing cement consumption in mortars by waste-derived hydrochars. *Journal of Building Engineering*, 75. doi:10.1016/j.jobbe.2023.106987.
- [2] Pachana, P. K., Rattanasak, U., Jitsangiam, P., & Chindaprasirt, P. (2021). Alkali-activated material synthesized from palm oil fuel ash for Cu/Zn ion removal from aqueous solutions. *Journal of Materials Research and Technology*, 13, 440–448. doi:10.1016/j.jmrt.2021.04.065.
- [3] Safiuddin, M., Salam, M. A., & Jumaat, M. Z. (2011). Utilization of palm oil fuel ash in concrete: A review. *Journal of Civil Engineering and Management*, 17(2), 234–247. doi:10.3846/13923730.2011.574450.
- [4] Abdeldjouad, L., Dheyab, W., Gamil, Y., Asadi, A., & Shukla, S. K. (2023). Thermal curing effects on alkali-activated treated soils with palm oil fuel ash. *Case Studies in Construction Materials*, 19, 532–539. doi:10.1016/j.cscm.2023.e02455.
- [5] Hawa, A., Salaemae, P., Abdulmatin, A., Ongwuttiwat, K., & Prachaseeree, W. (2023). Properties of Palm Oil Ash Geopolymer Containing Alumina Powder and Field Para Rubber Latex. *Civil Engineering Journal (Iran)*, 9(5), 1271–1288. doi:10.28991/CEJ-2023-09-05-017.
- [6] Liu, M. Y. J., Chua, C. P., Alengaram, U. J., & Jumaat, M. Z. (2014). Utilization of palm oil fuel ash as binder in lightweight oil palm shell geopolymer concrete. *Advances in Materials Science and Engineering*, 2014, 610274. doi:10.1155/2014/610274.
- [7] Runyut, D. A., Robert, S., Ismail, I., Ahmadi, R., & Abdul Samat, N. A. S. B. (2018). Microstructure and Mechanical Characterization of Alkali-Activated Palm Oil Fuel Ash. *Journal of Materials in Civil Engineering*, 30(7), 4018119. doi:10.1061/(asce)mt.1943-5533.0002303.
- [8] Mahamat Ahmat, A., Johnson, U.A., Fazaulnizam Shamsudin, M., Mahmoud Alnahhal, A., Shazril Idris Ibrahim, M., Ibrahim, S., & Rashid, R.S.M. (2023). Assessment of sustainable eco-processed pozzolan (EPP) from palm oil industry as a fly ash replacement in geopolymer concrete. *Construction and Building Materials*, 387, 131424. doi:10.1016/j.conbuildmat.2023.131424.
- [9] Najimi, M., Ghafoori, N., & Sharbaf, M. (2018). Alkali-activated natural pozzolan/slag mortars: A parametric study. *Construction and Building Materials*, 164, 625–643. doi:10.1016/j.conbuildmat.2017.12.222.
- [10] Ahmad, J., Kontoleon, K. J., Majdi, A., Naqash, M. T., Deifalla, A. F., Ben Kahla, N., Isleem, H. F., & Qaidi, S. M. A. (2022). A Comprehensive Review on the Ground Granulated Blast Furnace Slag (GGBS) in Concrete Production. *Sustainability (Switzerland)*, 14(14), 8783. doi:10.3390/su14148783.
- [11] Özbay, E., Erdemir, M., & Durmuş, H. I. (2016). Utilization and efficiency of ground granulated blast furnace slag on concrete properties - A review. *Construction and Building Materials*, 105, 423–434. doi:10.1016/j.conbuildmat.2015.12.153.

- [12] Blotevogel, S., Doussang, L., Poirier, M., André, L., Canizarès, A., Simon, P., ... & Cyr, M. (2024). The influence of Al₂O₃, CaO, MgO and TiO₂ content on the early-age reactivity of GGBS in blended cements, alkali-activated materials and supersulfated cements. *Cement and Concrete Research*, 178, 107439. doi:10.1016/j.cemconres.2024.107439.
- [13] Kumar, G., & Mishra, S. S. (2021). Effect of GGBFS on workability and strength of alkali-activated geopolymer concrete. *Civil Engineering Journal (Iran)*, 7(6), 1036–1049. doi:10.28991/cej-2021-03091708.
- [14] Sunarsih, E. S., As'ad, S., Sam, A. R. M., & Kristiawan, S. A. (2023). Properties of Fly Ash-Slag-Based Geopolymer Concrete with Low Molarity Sodium Hydroxide. *Civil Engineering Journal (Iran)*, 9(2), 381–392. doi:10.28991/CEJ-2023-09-02-010.
- [15] Tanu, H. M., & Unnikrishnan, S. (2023). Mechanical Strength and Microstructure of GGBS-SCBA based Geopolymer Concrete. *Journal of Materials Research and Technology*, 24, 7816–7831. doi:10.1016/j.jmrt.2023.05.051.
- [16] Bawab, J., El-Dieb, A., El-Hassan, H., & Khatib, J. (2023). Effect of different activation techniques on the engineering properties of cement-free binder containing volcanic ash and calcium carbide residue. *Construction and Building Materials*, 408, 133734. doi:10.1016/j.conbuildmat.2023.133734.
- [17] Abdulmatin, A., Khongpermgason, P., Jaturapitakkul, C., & Tangchirapat, W. (2018). Use of Eco-Friendly Cementing Material in Concrete Made from Bottom Ash and Calcium Carbide Residue. *Arabian Journal for Science and Engineering*, 43(4), 1617–1626. doi:10.1007/s13369-017-2685-x.
- [18] Rattanasotinunt, C., Tangchirapat, W., Jaturapitakkul, C., Cheewaket, T., & Chindaprasirt, P. (2018). Investigation on the strength, chloride migration, and water permeability of eco-friendly concretes from industrial by-product materials. *Journal of Cleaner Production*, 172, 1691–1698. doi:10.1016/j.jclepro.2017.12.044.
- [19] Dueramae, S., Tangchirapat, W., Chindaprasirt, P., & Jaturapitakkul, C. (2017). Influence of Activation Methods on Strength and Chloride Resistance of Concrete Using Calcium Carbide Residue–Fly Ash Mixture as a New Binder. *Journal of Materials in Civil Engineering*, 29(4), 4016265. doi:10.1061/(asce)mt.1943-5533.0001808.
- [20] Dueramae, S., Tangchirapat, W., Sukontasukkul, P., Chindaprasirt, P., & Jaturapitakkul, C. (2019). Investigation of compressive strength and microstructures of activated cement free binder from fly ash-calcium carbide residue mixture. *Journal of Materials Research and Technology*, 8(5), 4757–4765. doi:10.1016/j.jmrt.2019.08.022.
- [21] Hanjitsuwan, S., Phoo-ngernkham, T., & Damrongwiriyanupap, N. (2017). Comparative study using Portland cement and calcium carbide residue as a promoter in bottom ash geopolymer mortar. *Construction and Building Materials*, 133, 128–134. doi:10.1016/j.conbuildmat.2016.12.046.
- [22] Suttiprapa, P., Tangchirapat, W., Jaturapitakkul, C., Rattanasak, U., & Jitsangiam, P. (2021). Strength behavior and autogenous shrinkage of alkali-activated mortar made from low-calcium fly ash and calcium carbide residue mixture. *Construction and Building Materials*, 312, 125438. doi:10.1016/j.conbuildmat.2021.125438.
- [23] Li, Z., & Ikeda, K. (2023). Influencing Factors of Sulfuric Acid Resistance of Ca-Rich Alkali-Activated Materials. *Materials*, 16(6), 2473. doi:10.3390/ma16062473.
- [24] Jeon, I. K., Qudoos, A., Jakhriani, S. H., Kim, H. G., & Ryou, J. S. (2020). Investigation of sulfuric acid attack upon cement mortars containing silicon carbide powder. *Powder Technology*, 359, 181–189. doi:10.1016/j.powtec.2019.10.026.
- [25] Aliques-Granero, J., Tognonvi, T. M., & Tagnit-Hamou, A. (2017). Durability test methods and their application to AAMs: case of sulfuric-acid resistance. *Materials and Structures/Materiaux et Constructions*, 50(1), 1–14. doi:10.1617/s11527-016-0904-7.
- [26] ASTM C989/C989-22. (2024). Standard Specification for Slag Cement for Use in Concrete and Mortars. ASTM International, Pennsylvania, United States. doi:10.1520/C0989_C0989M-22.
- [27] Chang, J. J. (2003). A study on the setting characteristics of sodium silicate-activated slag pastes. *Cement and Concrete Research*, 33(7), 1005–1011. doi:10.1016/S0008-8846(02)01096-7.
- [28] Horpibulsuk, S., Phetchuay, C., Chinkulkijniwat, A., & Cholphatsorn, A. (2013). Strength development in silty clay stabilized with calcium carbide residue and fly ash. *Soils and Foundations*, 53(4), 477–486. doi:10.1016/j.sandf.2013.06.001.
- [29] Kampala, A., Horpibulsuk, S., Chinkulkijniwat, A., & Shen, S. L. (2013). Engineering properties of recycled Calcium Carbide Residue stabilized clay as fill and pavement materials. *Construction and Building Materials*, 46, 203–210. doi:10.1016/j.conbuildmat.2013.04.037.
- [30] Somna, K., Jaturapitakkul, C., & Kajitvichyanukul, P. (2011). Microstructure of Calcium Carbide Residue–Ground Fly Ash Paste. *Journal of Materials in Civil Engineering*, 23(3), 298–304. doi:10.1061/(asce)mt.1943-5533.0000167.
- [31] ASTM C109/C109M-20. (2020). Standard Test Method for Compressive Strength of Hydraulic Cement Mortars (Using 2-in. or [50-mm] Cube Specimens). ASTM International, Pennsylvania, United States. doi:10.1520/C0109_C0109M-20.
- [32] Dueramae, S., Sanboonsiri, S., Suntadyon, T., Aoudta, B., Tangchirapat, W., Jongpradist, P., Pulngern, T., Jitsangiam, P., & Jaturapitakkul, C. (2021). Properties of lightweight alkali activated controlled Low-Strength material using calcium carbide residue – Fly ash mixture and containing EPS beads. *Construction and Building Materials*, 297, 123769. doi:10.1016/j.conbuildmat.2021.123769.

- [33] Norrarat, P., Tangchirapat, W., Songpiriyakij, S., & Jaturapitakkul, C. (2019). Evaluation of Strengths from Cement Hydration and Slag Reaction of Mortars Containing High Volume of Ground River Sand and GGBF Slag. *Advances in Civil Engineering*, 2019, 4892015. doi:10.1155/2019/4892015.
- [34] Castellano, C. C., Bonavetti, V. L., Donza, H. A., & Irassar, E. F. (2016). The effect of w/b and temperature on the hydration and strength of blastfurnace slag cements. *Construction and Building Materials*, 111, 679–688. doi:10.1016/j.conbuildmat.2015.11.001.
- [35] Rattanasak, U., & Chindapasirt, P. (2009). Influence of NaOH solution on the synthesis of fly ash geopolymer. *Minerals Engineering*, 22(12), 1073–1078. doi:10.1016/j.mineng.2009.03.022.
- [36] Memon, F. A., Nuruddin, M. F., Khan, S., Shafiq, N., & Ayub, T. (2013). Effect of sodium hydroxide concentration on fresh properties and compressive strength of self-compacting geopolymer concrete. *Journal of Engineering Science and Technology*, 8(1), 44–56.
- [37] Lee, W. K. W., & Van Deventer, J. S. J. (2002). The effects of inorganic salt contamination on the strength and durability of geopolymers. *Colloids and Surfaces A: Physicochemical and Engineering Aspects*, 211(2–3), 115–126. doi:10.1016/S0927-7757(02)00239-X.
- [38] Alonso, S., & Palomo, A. (2001). Alkaline activation of metakaolin and calcium hydroxide mixtures: Influence of temperature, activator concentration and solids ratio. *Materials Letters*, 47(1–2), 55–62. doi:10.1016/S0167-577X(00)00212-3.
- [39] Dueramae, S., Tangchirapat, W., & Jaturapitakkul, C. (2018). Strength and heat generation of concrete using carbide lime and fly ash as a new cementitious material without Portland cement. *Advanced Powder Technology*, 29(3), 672–681. doi:10.1016/j.apt.2017.12.007.
- [40] Sata, V., Sathonsaowaphak, A., & Chindapasirt, P. (2012). Resistance of lignite bottom ash geopolymer mortar to sulfate and sulfuric acid attack. *Cement and Concrete Composites*, 34(5), 700–708. doi:10.1016/j.cemconcomp.2012.01.010.
- [41] Teymouri, M., Behfarnia, K., Shabani, A., & Saadatian, A. (2022). The Effect of Mixture Proportion on the Performance of Alkali-Activated Slag Concrete Subjected to Sulfuric Acid Attack. *Materials*, 15(19), 6754. doi:10.3390/ma15196754.
- [42] Yusuf, M. O., Megat Johari, M. A., Ahmad, Z. A., & Maslehuddin, M. (2015). Evaluation of Slag-Blended Alkaline-Activated Palm Oil Fuel Ash Mortar Exposed to the Sulfuric Acid Environment. *Journal of Materials in Civil Engineering*, 27(12), 4015058. doi:10.1061/(asce)mt.1943-5533.0001315.
- [43] Bakharev, T. (2005). Resistance of geopolymer materials to acid attack. *Cement and Concrete Research*, 35(4), 658–670. doi:10.1016/j.cemconres.2004.06.005.
- [44] Allahverdi, A., & Skvara, F. (2006). Sulfuric acid attack on hardened paste of geopolymer cements-part 2. Corrosion mechanism at mild and relatively low concentrations. *Ceramics Silikaty*, 50(1), 1.
- [45] Gijbels, K., Pontikes, Y., Samyn, P., Schreurs, S., & Schroyers, W. (2020). Effect of NaOH content on hydration, mineralogy, porosity and strength in alkali/sulfate-activated binders from ground granulated blast furnace slag and phosphogypsum. *Cement and Concrete Research*, 132, 106054. doi:10.1016/j.cemconres.2020.106054.
- [46] Fu, Q., Bu, M., Zhang, Z., Xu, W., Yuan, Q., & Niu, D. (2023). Hydration Characteristics and Microstructure of Alkali-Activated Slag Concrete: A Review. *Engineering*, 20, 162–179. doi:10.1016/j.eng.2021.07.026.
- [47] Khater, H. M. (2012). Effect of Calcium on Geopolymerization of Aluminosilicate Wastes. *Journal of Materials in Civil Engineering*, 24(1), 92–101. doi:10.1061/(asce)mt.1943-5533.0000352.
- [48] Walkley, B., San Nicolas, R., Sani, M. A., Rees, G. J., Hanna, J. V., van Deventer, J. S. J., & Provis, J. L. (2016). Phase evolution of C-(N)-A-S-H/N-A-S-H gel blends investigated via alkali-activation of synthetic calcium aluminosilicate precursors. *Cement and Concrete Research*, 89, 120–135. doi:10.1016/j.cemconres.2016.08.010.
- [49] Liu, Q., Zhang, J., Su, Y., & Lü, X. (2021). Variation in Polymerization Degree of C-A-S-H Gels and Its Role in Strength Development of Alkali-activated Slag Binders. *Journal of Wuhan University of Technology, Materials Science Edition*, 36(6), 871–879. doi:10.1007/s11595-021-2281-z.
- [50] Huang, Z., Zhou, Y., & Cui, Y. (2021). Effect of Different NaOH Solution Concentrations on Mechanical Properties and Microstructure of Alkali-Activated Blast Furnace Ferronickel Slag. *Crystals*, 11(11), 1301. doi:10.3390/cryst11111301.
- [51] Irshidat, M. R., Al-Nuaimi, N., & Rabie, M. (2021). Sustainable utilization of waste carbon black in alkali-activated mortar production. *Case Studies in Construction Materials*, 15, 743. doi:10.1016/j.cscm.2021.e00743.
- [52] Zhang, H. Y., Kodur, V., Wu, B., Cao, L., & Qi, S. L. (2016). Comparative Thermal and Mechanical Performance of Geopolymers derived from Metakaolin and Fly Ash. *Journal of Materials in Civil Engineering*, 28(2), 4015092. doi:10.1061/(asce)mt.1943-5533.0001359.

- [53] Tai, Z. S., Hubadillah, S. K., Othman, M. H. D., Dzahir, M. I. H. M., Koo, K. N., Tendot, N. I. S. T. I., Ismail, A. F., Rahman, M. A., Jaafar, J., & Aziz, M. H. A. (2019). Influence of pre-treatment temperature of palm oil fuel ash on the properties and performance of green ceramic hollow fiber membranes towards oil/water separation application. *Separation and Purification Technology*, 222, 264–277. doi:10.1016/j.seppur.2019.04.046.
- [54] Haha, M. Ben, Lothenbach, B., Le Saout, G., & Winnefeld, F. (2012). Influence of slag chemistry on the hydration of alkali-activated blast-furnace slag - Part II: Effect of Al₂O₃. *Cement and Concrete Research*, 42(1), 74–83. doi:10.1016/j.cemconres.2011.08.005.
- [55] El-Jazairi, B., & Illston, J. M. (1977). A simultaneous semi-isothermal method of thermogravimetry and derivative thermogravimetry, and its application to cement pastes. *Cement and Concrete Research*, 7(3), 247–257. doi:10.1016/0008-8846(77)90086-2.
- [56] Men, S., Tangchirapat, W., Jaturapitakkul, C., & Ban, C. C. (2022). Strength, fluid transport and microstructure of high-strength concrete incorporating high-volume ground palm oil fuel ash blended with fly ash and limestone powder. *Journal of Building Engineering*, 56, 104714. doi:10.1016/j.jobbe.2022.104714.
- [57] Kulasuriya, C., Dias, W. P. S., Vimonsatit, V., & De Silva, P. (2020). Mechanical and Microstructural Properties of Alkali Pozzolan Cement (APC). *International Journal of Civil Engineering*, 18(11), 1281–1292. doi:10.1007/s40999-020-00534-3.
- [58] Guo, W., Zhang, Z., Bai, Y., Zhao, G., Sang, Z., & Zhao, Q. (2021). Development and characterization of a new multi-strength level binder system using soda residue-carbide slag as composite activator. *Construction and Building Materials*, 291, 123367. doi:10.1016/j.conbuildmat.2021.123367.
- [59] Chen, K., Lin, W. T., & Liu, W. (2021). Effect of NaOH concentration on properties and microstructure of a novel reactive ultra-fine fly ash geopolymer. *Advanced Powder Technology*, 32(8), 2929–2939. doi:10.1016/j.appt.2021.06.008.